Quaternary Science Reviews 359 (2025) 109346

Contents lists available at ScienceDirect

Quaternary Science Reviews

journal homepage: www.elsevier.com/locate/quascirev

Explosive volcanic history of Snæfellsjökull, West Iceland: Geochemistry, chronology and tephra distribution

Wesley R. Farnsworth [a,b,*], Nína Aradóttir [a], Skafti Brynjólfsson [c], Sigrún D. Eddudóttir [d], Egill Erlendsson [d], Guðmundur H. Guðfinnsson [a], Esther R. Guðmundsdóttir [a], Maarit Kalliokoski [e], Guðrún Larsen [a], Rebekka H. Rúnarsdóttir [a], Anthony H. Ruter [b], Marie-Louise Siggaard-Andersen [b], Sveinbjörn Steinþórsson [a], Nicolaj K. Larsen [b], Kurt H. Kjær [b]

[a] NordVulk, Institute of Earth Sciences, University of Iceland, Askja, Sturlugata 7, IS-102, Reykjavík, Iceland
[b] Globe Institute, University of Copenhagen, Øster Voldgade 5-7, DK-1350, Copenhagen K., Denmark
[c] Icelandic Institute of Natural History, Borgum við Norðurslóð, IS-600, Akureyri, Iceland
[d] The Icelandic Agricultural Advisory Center, Höfdabakki 9, Reykjavik, IS-110, Iceland
[e] Dept. of Geography and Geology, University of Turku, 20014, Turun yliopisto, Finland

ARTICLE INFO

Handling editor: Giovanni Zanchetta

Keywords:
Cryptotephra
Lake record
Volcanicum hazard
Isochron

ABSTRACT

Tephrochronology is firmly rooted in our knowledge of volcanic history. Iceland's Holocene explosive volcanic history is predominantly derived from investigations of soil sections and written archives, following the Norse Settlement *c.* 877 CE. Unsurprisingly, historically active volcanic provinces are most often the target of these tephrochronological investigations (e.g., Hekla, Katla, Bárðarbunga-Veiðivötn and Grímsvötn). Despite the risk of large explosive eruptions, some volcanic provinces – like Snæfellsjökull have received less attention. While no historical eruptions have been described from the glaciated central volcano, mapping from the late 1960s and early 1980s suggests there have been at least three explosive eruptions (producing silicic tephra) during the Holocene: Sn-1 (~1.8 ka BP), Sn-2 (~4.4 ka BP) and Sn-3 (~8–10 ka BP). The presence of at least two of these tephra layers in European stratigraphic records has been suggested. Furthermore, other (cryptotephra) horizons in Europe exhibit similar geochemical properties to the Snæfellsjökull province, albeit different age estimates than Sn-1, -2, or -3. The tephrochronological potential of Snæfellsjökull tephra is limited by our lack of fundamental knowledge on the volcanic history and the potential range in tephra geochemistry from this stratovolcano. As a step towards addressing this knowledge gap, we present a well-dated record of tephra stratigraphy from lake Laugarvatn, near Snæfellsjökull. Furthermore, we review all Snæfellsjökull-like tephra deposits to improve understanding of Snæfellsjökull's post-glacial explosive volcanic activity affecting both regional and distal environments.

1. Introduction

Tephrochronology has the potential to be the most robust, precise and widespread geochronological constraint to geological archives. However, the technique's value is directly dependent on our understanding of the geochemical composition of tephra produced by explosive eruptions of various volcanoes, the eruption age and tephra distribution. Understanding the volcanic history and, specifically, the frequency and magnitude of past explosive eruptions, is critically important for gauging the reoccurrence interval and likelihood of future eruptions (e.g., Larsen and Eiríksson, 2008).

The partly glaciated volcanic island of Iceland is the largest contributor to North Atlantic tephra production and its post-settlement (c. 877 CE onwards) volcanic history is well documented (Fig. 1; Þorarinsson, 1958, 1967, 1981; Larsen, 1984, 2000; Þórðarson and Self, 2003; Larsen et al., 1999; Hafliðason et al., 2000; Carey et al., 2010; Sigurgeirsson et al., 2013; Schmid et al., 2017). Understanding of Iceland's prehistoric explosive volcanic history is largely derived from

* Corresponding author. NordVulk, Institute of Earth Sciences, University of Iceland, Askja, Sturlugata 7, IS-102, Reykjavík, Iceland.
E-mail address: wesleyF@hi.is (W.R. Farnsworth).

https://doi.org/10.1016/j.quascirev.2025.109346
Received 28 October 2024; Received in revised form 11 February 2025; Accepted 30 March 2025
Available online 23 April 2025

stratigraphic investigations of interbedded soil and tephra (Þorarinsson, 1944; Larsen and Thorarinsson, 1977; Jóhannesson et al., 1981; Larsen et al., 2001, 2002; Óladóttir et al. 2005, 2008, 2011a, 2011b; Larsen and Eiríksson, 2008; Guðmundsdóttir et al., 2011, 2016). Soil investigations allow for the mapping of tephra isopach contours and the depositional axis of tephra fallout by correlating characteristically similar tephra layers and their thickness, spatially (e.g., Þorarinsson, 1967; Jóhannesson et al., 1981). While this approach provides detail to our understanding of past explosive volcanism, it is limited by the development, stability and distribution of soil (Dugmore and Sugden, 1991; Dugmore et al., 2009; Andrade et al., 2021). Lake archives are more frequently being used for a better understanding of volcanic history as a supplement to soil archives (e.g., Björck et al., 1992; Jóhannsdóttir, 2007; Larsen et al., 2012; Striberger et al., 2012; Guðmundsdóttir et al., 2016, 2018; Harning et al., 2016, 2019; Andrade et al., 2021). Although lake investigations generally consist of fewer specific data points (compared to soil section mapping), lake records, in theory, exhibit continuous sedimentation. Additionally, they record time intervals pre-dating establishment of widespread soil archives, when land-based accumulation may have been irregular or non-existent (Björck et al.,

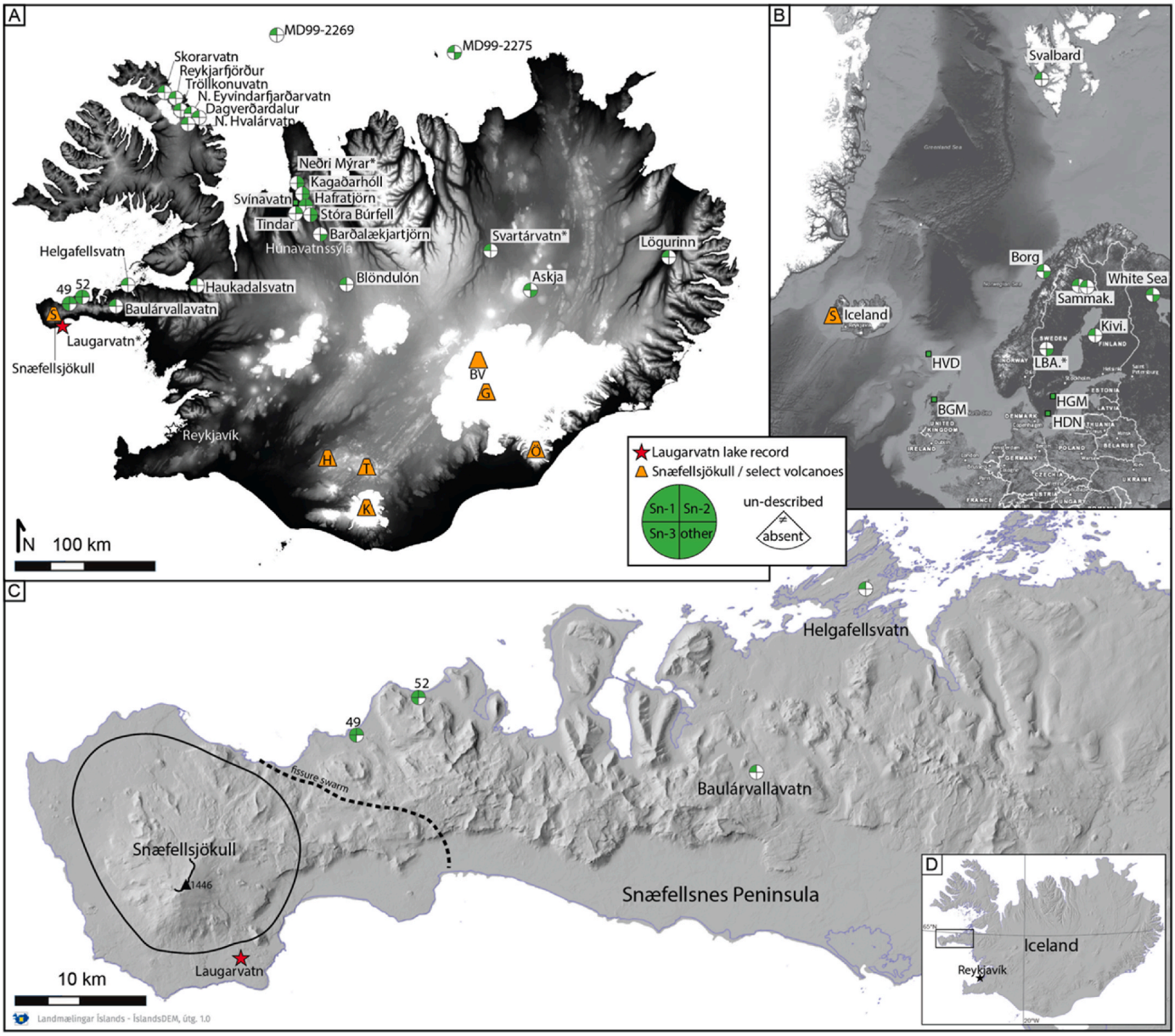

Fig. 1. A) Digital elevation model of Iceland showing selected volcanic provinces and records with published Snæfellsjökull tephra. Volcanic provinces H = Hekla; K = Katla; T = Torfajökull; G = Grímsvötn; BV = Bárðarbunga-Veiðivötn; Ö = Öræfajökull. B) Map of the North Atlantic showing the location of Iceland and the Snæfellsjökull volcano as well as distal records with published Snæfellsjökull tephra. Green boxes mark locations with suggested Snæfellsjökull tephra discussed in the text. Site names and records; Svalbard = Kongressvatn, Spitsbergen; Borg = Borg Bog, Lofoten; Sammak = Sammakovuoma, Sweden; White Sea = Vodoprovodnoe, White Sea; Kivi = Kivihypönneva, Finland; LBA = Lilla Backsjömyren, Sweden; HVD = Hovsdalur, Faroes; BGM = Ben Goram Moss, Scotland; HGM = Högstorpsmossen, Sweden; and HDN = Hässeldalen, Sweden (Table 2), C) Hill-shade map of Snæfellsnes peninsula showing Snæfellsjökull fissure swarm, central volcano and caldera rim (Jóhannesson and Sæmundsson, 1998; Jóhannesson 2013; 2019). The location of lake Laugarvatn is indicated by a red star. Sites 49 and 52 are two of the 91 soil sections logged by Jóhannesson et al. (1981) referred to in this study. D) Inset map of Iceland showing the location of Snæfellsnes peninsula in relation to capital city, Reykjavík. Complete list of site names and references reported in Table 2, Section 3. The * follow site names in *Neðri Mýrar* and *Svartárvatn* in map A) and *LBA* in map B) mark sites where Snæfellsjökull tephra has been dated (Table S2). (For interpretation of the references to color in this figure legend, the reader is referred to the Web version of this article.)

1992; Andrade et al., 2021).

In Iceland, tephrochronological investigations through the last century have mainly focused on historically active volcanic provinces (e.g., Hekla, Katla, Öræfajökull, Bárðarbunga-Veiðivötn and Grímsvötn), leaving some volcanic provinces less studied (Fig. 1). Furthermore, knowledge gaps exist in relation to specific understudied coastal provinces (largely flanked by sea rather than land or soil archive), despite the possible risk of explosive eruptions (volcanic explosivity index, VEI $\geq$4; Newhall and Self, 1982), capable of impacting large parts of the Northern Hemisphere. The Snæfellsjökull volcano, located on a peninsula extending 100 km off the west coast of Iceland (located 110 km from Reykjavík), is a prime example of one of these less studied provinces (Fig. 1). Regional mapping on the peninsula, from the late 1960s, and early 1980s indicates the distribution of three tephra layers from Snæfellsjökull explosive eruptions (Sigurðsson, 1966; Steinþórsson, 1967; Jóhannesson et al., 1981). However, other tephra layers identified at numerous locations in Iceland, as well as in Northern Europe, have also been suggested to originate from Snæfellsjökull (Fig. 1; Sigvaldason et al., 1992; Langdon and Barber, 2001; Wastegård et al., 2009; Eddudóttir et al., 2015, 2016; Holmes et al., 2016; Tinganelli et al., 2018; Vakhrameeva et al., 2020; Bates et al., 2022). Ultimately, we lack fundamental knowledge on the extent of post-glacial explosive volcanism from Snæfellsjökull and the compositional range in tephra geochemistry.

Here we compile, curate and synthesize the state-of-the-art knowledge on tephra from the Snæfellsjökull volcanic system. We re-analyzed Sn-1, -2 and -3 (Sites 49 and 52 as described by Jóhannesson et al., 1981) to establish a proximal, up-to-date geochemical composition of the three previously described silicic tephra layers. Furthermore, we analyzed tephra from lake Laugarvatn located on the southwest extent of the Snæfellsnes peninsula, proximal to the Snæfellsjökull strato-volcano, to supplement the early mapping by Jóhannesson et al. (1981). The new, well-dated lake sediment archive contains 17 tephra layers originating from the Snæfellsjökull province and enhances our understanding of its volcanic history over the last 10,000 years. Our data are summarized and compared to Snæfellsjökull tephra described from sites across Iceland and Northern Europe. This review, along with our new data, furthers our knowledge on the distribution of Snæfellsjökull tephra, the geochemical composition of the glass, as well as the age of the deposits. This basic research is valuable for improving the North Atlantic tephrochronological framework. Furthermore, this fundamental knowledge is key for defining reoccurrence intervals and estimating the likelihood and type of future eruptions at Snæfellsjökull.

1.1. Geological setting

Iceland is a volcanic island located in the middle of the North Atlantic on a subaerially exposed microcontinent of the Mid-Atlantic Ridge (Einarsson, 2008; Sigmundsson et al., 2020; Foulger et al., 2020). The island rises over 2 km from sea level and has formed through the interactions of the ongoing rifting at the mid-oceanic ridge and extensive mantle upwelling (Sigmundsson et al., 2022; Halldórsson et al., 2022). The oldest strata (*c.* 16 Ma) are located in the northwest and east of Iceland; however, the island continues to form as a result of the ongoing divergence of the North American and Eurasian plates, as well as the active volcanism (Denk et al., 2011; Wright et al., 2012; Sigmundsson et al., 2022). Iceland hosts ~32 volcanic systems with many of them active today (Sigmundsson et al., 2020; Catalogue of Icelandic Volcanos: https://icelandicvolcanos.is/). The Snæfellsnes volcanic zone is the westernmost province and extends WNW-ESE on the outermost portion of the Snæfellsnes peninsula (Fig. 1; Jóhannesson, 2019). The central volcano's oldest rocks are believed to be *c.* 800 ka BP and unconformably overlie and eroded the Tertiary basement (Jóhannesson, 1980; Jóhannesson et al., 1981, 2019).

1.2. Snæfellsjökull volcanism and tephra distribution

An estimated 20–25 Holocene eruptions have been proposed for the Snæfellsjökull volcanic system. Most of these eruptions were effusive, producing basaltic-intermediate lava flows (located on the south and western slopes), which extend between 5 and 7 km and cover areas between 4 and 18 km^2 (Fig. 2B; Jóhannesson, 2019; Harðarson, 1993). The larger lava flows are of intermediate composition, originating from the Snæfellsjökull summit area, exhibiting flow lengths up to 8-km and areal extent up to ~30 km^2 (with volumes up to 0.5 km^3; Jóhannesson, 2019). In the absence of documentation of post-settlement volcanism from the region, all Snæfellsjökull eruptions and lava flows are believed to be pre-Historic (Fig. 2b; Jóhannesson et al., 1981; Harðarson, 1993).

Three explosive eruptions have been described from the post-glacial era: Sn-1 (~1.8 ka BP), Sn-2 (~4.4 ka BP) and Sn-3 (~8–10 ka BP; Sigurðsson, 1966; Steinþórsson, 1967; Jóhannesson et al., 1981; Jóhannesson, 1982a, b). Jóhannesson et al. (1981, 1982a, b) correlated the youngest two of these eruptions to local bulk radiocarbon ages presented by Steinþórsson (1967; Table 1) and estimated the age of Sn-3 based on its early (lower) stratigraphic positioning, over a diamict. Stratigraphic investigations of soil sections from the Snæfellsnes peninsula (dominantly located on the northern half), suggest tephra deposition (isopach orientation) towards the ENE for the three silicic tephra layers (Sigurðsson, 1966; Flores, 1981; Jóhannesson et al., 1981). Tephra volumes are estimated to 0.2–0.5 km^3, equating to a VEI 4 (Jóhannesson, 2019).

Proximal lake sediment records from the Snæfellsnes peninsula support the soil isopach trajectory for the most recent eruption, as Sn-1 has been identified in Helgafellsvatn, 22 m a.s.l. (Riddell et al., 2024) and Baulárvallavatn, 194 m a.s.l. (Holmes et al., 2016). Tephra geochemistry from Snæfellsnes indicates intermediate-silicic composition (~65–69 SiO_2 wt%) for Sn-1 with a characteristically high Al_2O_3 content (~16 wt %; Larsen et al., 2002).

Snæfellsjökull tephra has been described from over 20 sites (soil and lake archives) across northern Iceland (Fig. 1; Table 2). Furthermore, Snæfellsjökull tephra is described as diffuse layers from marine records on the shelf north of Iceland, as well as crypto-tephra layers from more than seven sites in Northern Europe and the Arctic, including Svalbard, Norway, Sweden, Finland and Western Russia (Fig. 1; Table 2). The Sn-1 tephra is the most widely identified and correlated tephra layer. The marker layer has been described from 22 sites in Iceland and overseas, in addition to the ~20 sites logged by Jóhannesson et al. (1981) on the Snæfellsnes peninsula. The Sn-2 tephra has been identified at six locations in Iceland (mainly Húnavatnssýsla), in addition to the ~70 sites (on Snæfellsnes peninsula) described by Jóhannesson et al. (1981). However, it has not yet been described from stratigraphic archives overseas (Fig. 1; Table 2). Finally, Sn-3 has not been described from beyond the Snæfellsnes peninsula, likely resulting from the unknown geochemistry, age uncertainty and relatively few Icelandic soil records extending back into the Early Holocene.

Additionally, several tephra layers have been described from Iceland and Northern Europe exhibiting similar evolved geochemical composition to Snæfellsjökull tephra but with unknown origins. In publications, these tephra layers are either: 1) associated with another more active province like Hekla; 2) attributed to Snæfellsjökull – correctly; or 3) attributed to Snæfellsjökull – incorrectly. For example, the HUN tephra described from Húnavatnssýsla, Iceland (Eddudóttir et al., 2016; Bates et al., 2022), is believed to be 5.5 cal ka BP with intermediate composition and was originally suggested to derive from Hekla (Eddudóttir et al., 2016). Additionally, stratigraphic work in the mid-1980s described a silicic tephra layer (*tephra x*) positioned between Hekla 3 and Hekla 4 in the Askja region of Iceland (Annertz et al., 1985; Sigvaldasson et al. 1993). A similar cryptotephra layer was described from Sweden (LBA-2) and was well dated to a similar age of 3.6 cal ka BP. Both these layers present similar composition which is comparable to Sn-1 (Wastegård et al., 2009). From here on, we refer to these tephra

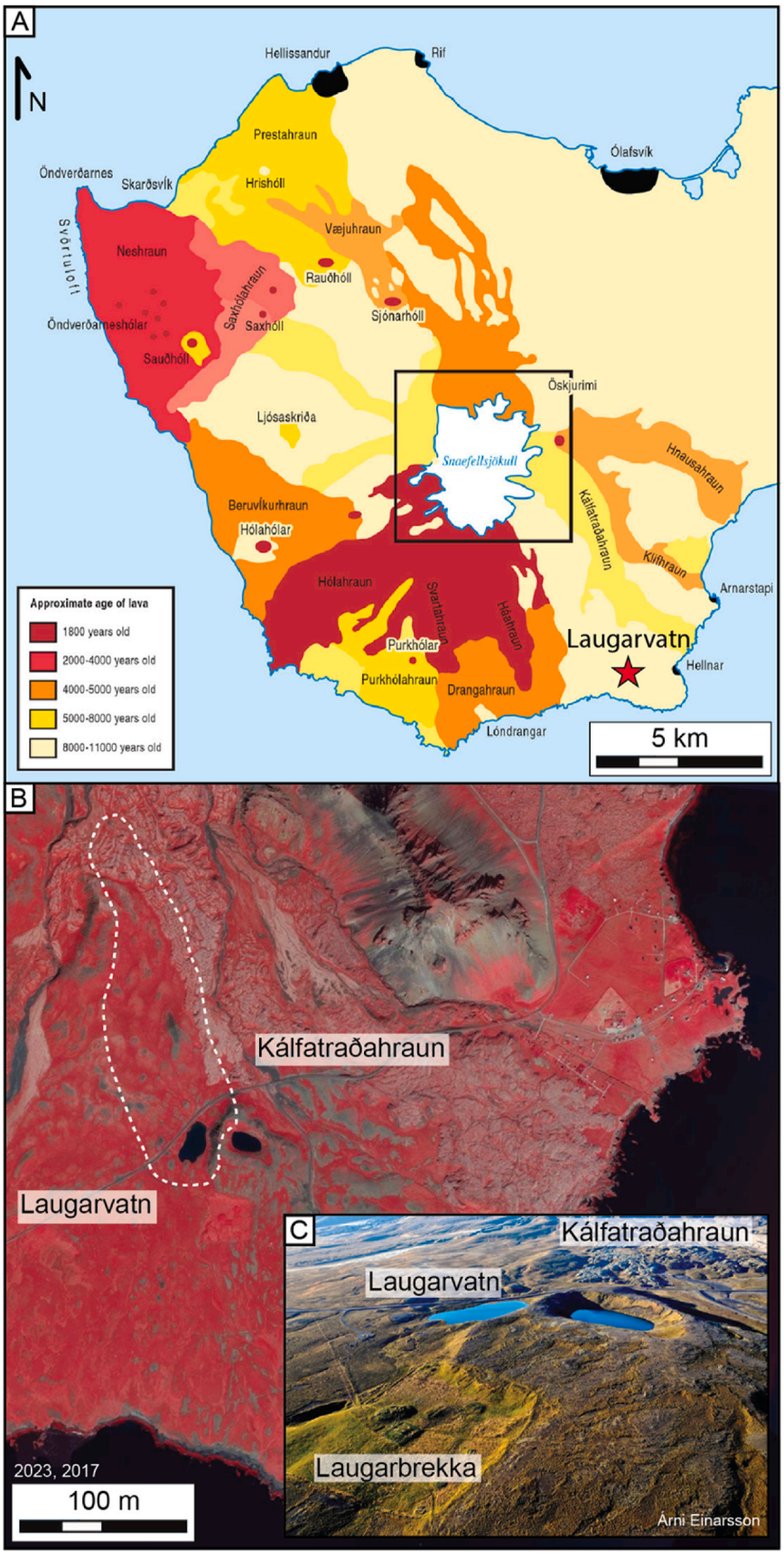

(caption on next page)

Fig. 2. A) Map (modified from Evans et al., 2016) of prehistoric lava flows, with approximate ages encompassing the Snæfellsjökull volcano (Harðarson, 1993; Jóhannesson et al., 1981). B) Infrared satellite image mosaic (2023 and 2017) from the Laugarvatn region with approximate catchment indicated by a dashed line (Map.is Database, 2024; Loftmyndir, 2017; 2023). C) Oblique aerial image of Laugarvatn, located at 76 m a.s.l. on the southwest side of Snæfellsnes peninsula, Iceland. The Kálfatraðahraun lava, 5–8 cal. ka BP enters the northern extent of the Laugarvatn lake catchment. Remnants of the Laugarbrekka farm are visible in the foreground (drone image courtesy of Árni Einarsson).

layers as Sn-H and Sn-X.

Younger Snæfellsjökull-like tephra has been described from the marine core MD99-2275 collected north of Iceland. At this site on the shelf, two distinct, albeit low concentration, layers of tephra were identified with Sn-1 composition (Larsen et al., 2002). Ultimately the deeper and more prominent horizon was used as the marker layer (Guðmundsdóttir et al., 2012). Snæfellsjökull tephra has also been described from "historical" sediments in Norway and the White Sea Region (i.e. after the Settlement of Iceland; Pilcher et al., 2005; Vakhrameeva et al., 2020). It has been suggested that these two records exhibit Snæfellsjökull tephra stratigraphically above the distally deposited basaltic component of the Landnám tephra layer (877 AD; Table 2). Finally, there are several other tephra layers – from an unknown province – (e.g., *Högstorpsmossen*, Björck and Wastegård, 1999; *Hässeldalen*, Davies et al., 2003; *Ben Goram Moss*, Langdon and Barber, 2001) where Snæfellsjökull has been suggested a possible source. Correlation has been hampered, however, by our limited understanding of the Snæfellsjökull volcanic history. These tephra layers will be further discussed in Section 4.

1.3. Study sites

1.3.1. Soil sections

The Sections 49 and 52, first described by Jóhannesson et al. (1981), were revisited and re-sampled (Fig. 1A–C). The sections are located on the northern side of the peninsula, located roughly 15 and 20 km to the northeast of the Snæfellsjokull summit, respectively. The two sites are approximately 1.5-m (49) and 3-m (52) exposures of peat and soil with interbedded tephra. It was estimated that the upper two tephra layers were Late Holocene in age while the lowermost tephra was assumed to date to the Early Holocene (Jóhannesson et al., 1981).

1.3.2. Laugarvatn, SW Snæfellsnes

A composite lake record (composed of six cores from two sequential drives) was collected from the Laugarvatn lake basin (64.7584°N; 23.6866 °W), located on the southwest coast of the Snæfellsnes peninsula at *c.* 76 m a.s.l. The shallow (<2 m), 0.03 km^2 lake basin is situated roughly 1.7 km from the coast and *c.* 6.7 km southeast of the Snæfellsjökull summit (1446 m a.s.l.; Figs. 1D and 2). The lake catchment is *c.* 1.08 km^2 and partially contains some of the post-glacial, c. 5–8 ka BP *Kálfatraðahraun lava*, (Jóhannesson et al., 1981; Kokfelt et al., 2009). Notably, the deserted farmstead Laugarbrekka, birthplace of Guðríður þorbjarnardóttir, the first Norse woman to travel to North America, is located proximal to Laugarvatn (Crocker, 2023, Fig. 2). Archaeological remnants in the catchment area of Lake Laugarvatn and historical data suggest an early settlement (Crocker, 2023).

2. Methods

2.1. Soil section investigation

Tephra samples were collected from peaty soil at Sections 49 and 52 on Snæfellsnes (Jóhannesson et al., 1981). The sections were clean, logged and light-colored silicic tephra was re-sampled. This was conducted to provide updated analysis of the tephra layers Sn-1, Sn-2 and Sn-3. Four samples of three silicic tephra layers were collected (Fig. S1). At each section, two light-colored tephra layers were sampled interbedded within organic rich soil and peat. Proximal to Section 49, tephra layers Sn-1 (K-2; *c.* 8 cm thick) and Sn-2 (K-4; *c.* 9 cm thick and 25 cm beneath Sn-1) were sampled from the upper 0.75 m of a *c.* 1.5 m exposure. Proximal to Section 52, in an approximately 3 m peat section, Sn-3 (K-1; *c.* 6 cm) was sampled *c.* 1 m from the base of the sequence and Sn-1 (K-3; 10 cm) was sampled *c.* 1.5 m stratigraphically above it. At Site 52, Sn-2 was not sampled. The maker layer did not make up a prominent horizon in the section and was detected as only sporadic grains.

Furthermore, unpublished stratigraphic data (tephra and radiocarbon ages) from three previously described (Eddudóttir et al., 2016), peat sections in Húnavatnssýsla are discussed (Fig. S2; Doc S1). The Húnavatnssýsla sections Neðri Mýrar - NM, Kagaðarhóll - KAGAV and Stóra Búrfell - BUR, were cleaned and subsampled with monoliths in the field. The monoliths were taken side by side with overlapping intervals, often targeting a distinct layer (like Hekla 4). Visible tephra was sampled from the monoliths. Furthermore, non-visible tephra was identified and sampled by targeting peaks in magnetic susceptibility (which was measured at 1 cm resolution on the records (Fig. S2; Doc. S1).

2.2. Lake coring

A total of six lake sediment cores were recovered to develop a composite record from Laugarvatn. The cores were collected from the central basin (*c.* 1.6 m water depth) of Laugarvatn through lake ice in January and March 2022 (see Fig. S3). Two full sequences of strata were collected proximal to one another to construct a continuous overlapping record. Cores were taken in sequence with a lightweight piston-corer and 205-cm-long core tubes (70/64 mm diameter). The cores were transported to Denmark where they were split into "working" and "archive" core halves and prepared for laboratory analysis.

2.3. Core scanning

The archive core halves were analyzed in the sediment lab and ITRAX core facility at the Centre for GeoGenetics, Globe Institute, University of Copenhagen. The lithology and stratigraphy of the cores were visually inspected and logged. ITRAX scanning was run on each of the sediment cores to record visual and radiographic imagery, magnetic susceptibility, and X-ray fluorescence (XRF; Kylander et al., 2012). While correlations could be made visually, an approximately 580 cm-long composite lake core stratigraphy, ISL40x, was developed from the ITRAX core scan (Fig. S3).

2.4. Lake record geochronology

The working core halves were sampled to geochronologically constrain the sediment records. The chronological framework is built upon plutonium isotope analysis (Pu), radiocarbon dated macrofossils (^{14}C) and two known volcanic ash horizons (tephra).

2.4.1. Pu dating

To test the preservation of modern sediments at the sediment-water interface, six bulk sediment subsamples (taken every 3 cm) were collected from the uppermost 15 cm of the composite record (ISL22-17) for plutonium radiometric dating. Samples were run on an ICP-MS using a Thermo X2 quadrupole at the Northern Arizona University, following procedures adapted from Ketterer et al. (2004). Peak $Pu^{239+240}$ concentration is associated with nuclear weapons testing in 1963/1964 while the onset of global fall-out began 1952 (Kelley et al., 1999; Ketterer et al., 2002).

Table 1
Unnormalized ranges in electron microprobe geochemistry data of tephra sampled on Snæfellsnes peninsula from Sites 49 and 52 (Jóhannesson et al., 1981) as well as the Laugarvatn lake record. All probe analysis were conducted at the University of Iceland. Volcanic systems include: Torf. = Torfajökull; B-V = Bárðarbunga-Veiðivötn; Snæfells. = Snæfellsjökull. Composition according to total alkali-silica plot divisions: B = Basalt; TB = Trachy-basalt; BTA = Basaltic Trachy-andesite; TA = Trachy-andesite; TD = Trachydacite; R = Rhyolite. Marker layers[1] Landnám; 877 AD (1073 cal. BP; Larsen, 1984; Schmid et al., 2017),[2] Hekla-B; ~2800 cal. ka BP (Larsen et al., 2020) and[3] Hekla 4; 4325 ± 8 cal. ka BP (Davies et al., 2024) highlighted in grey.

Sample site	Sample ID	Volc. Province (Composition)	n =	SiO_2 (wt%)	TiO_2 (wt%)	Al_2O_3 (wt%)	FeO (wt%)	MnO (wt%)	MgO (wt%)	CaO (wt%)	Na_2O (wt %)	K_2O (wt%)	P_2O_5 (wt%)	Total (wt%)
Site 49	Sn-1 (K3)	**Snæfells. (TD)**	12	65.7–69.6	0.3–0.5	15.2–16.0	3.1–4.6	0.1–0.2	0.1–0.6	1.2–2.0	3.9–5.5	3.9–4.7	0.0–0.1	98.3–99.6
Site 52	Sn-1 (K2)	**Snæfells. (TD)**	14	65.3–70.0	0.2–0.6	14.7–16.0	3.0–5.0	0.1–0.2	0.1–0.5	1.0–2.2	5.1–5.4	3.8–4.7	0.0–0.1	96.1–99.3
Site 49	Sn-2 (K4)	**Snæfells. (TD)**	17	62.9–68.0	0.3–0.6	14.8–16.8	3.8-5-5	0.1–0.2	0.2–0.7	1.2-2-7	3.7–6.1	3.5–4.7	0.0–0.1	94.7–100.0
Site 52	Sn-3 (K1)	**Snæfells. (TA-TD)**	20	59.6–67.2	0.3–1.2	15.2–16.3	3.9–7.5	0.1–0.3	0.3–1.5	1.5–3.9	4.7–5.6	2.9–4.2	0.0–0.4	94.5–99.5
Laug.	ISL40x375[a]	**Torf. *Landnám*** [1] (R)	12	69.8–72.3	0.2–0.3	14.5–15.6	2.3–3.2	0.1–0.2	0.1–0.3	0.8–1.0	3.0–5.5	4.5–4.7	0.0–0.1	96.6–100.6
Laug.	ISL40x375[a]	**B-V *Landnám*** [1] (B)	3	49.2–49.8	1.8–1.8	13.8–14.0	12.5–13.2	0.2–0.3	6.5–6.5	10.9–11.4	2.2–2.5	0.2–0.2	0.2–0.2	98.4–99.4
Laug.	ISL40x655	**Snæfells. (BTA-TA)**	**11**	51.3–58.9	2.0–3.3	13.6–15.0	8.8–12.5	0.3–0.3	1.8–3.3	4.2–6.5	3.7–4.7	2.9–4.2	0.7–1.5	98.6–100.6
Laug.	ISL40x755	**Snæfells. (BTA-TD)**	**15**	55.2–68.6	0.3–2.5	14.1–16.5	3.5–10.3	0.2–0.3	0.2–2.4	1.4–5.5	4.3–5.4	2.8–5.2	0.1–1.0	98.5–100.5
Laug.	ISL40x788	**Snæfells. (BTA-TA)**	14	54.5–65.8	0.4–2.6	14.0–16.5	5.0–10.8	0.2–0.3	0.5–2.6	2.2–5.8	4.3–5.3	2.8–4.7	0.1–1.0	98.4–100.5
Laug.	ISL40x815[a]	**Snæfells. (BTA)**	11	55.0–57.5	2.1–2.6	14.1–14.7	9.1–11.0	0.2–0.3	2.1–2.6	4.6–5.8	4.0–4.9	2.8–3.9	0.7–1.1	98.5–99.7
Laug.	ISL40x1013	**Snæfells. (BTA-TA)**	28	52.3–64.7	0.7–2.8	13.7–16.0	6.4–11.7	0.2–0.3	0.7–2.7	2.3–6.2	4.2–5.8	2.7–4.3	0.2–1.3	97.7–100.2
Laug.	ISL40x1775	**Hekla *B*** [2] **(BTA-TA)**	15	53.6–63.4	0.8–2.2	13.8–16.1	7.0–12.9	0.2-0-3	1.3–3.2	4.3–6.8	2.7–4.4	1.2–1.7	0.3–1.3	98.4–100.2
Laug.	ISL40x1898[a]	**Snæfells. (BTA-TA)**	12	51.5–64.3	0.9–3.4	13.4–16.6	5.9–12.9	0.2–0.3	0.8–3.4	2.4–6.8	3.8–5.6	2.4–4.1	0.3–1.5	97.8–99.7
Laug.	ISL40x1988[b]	**Snæfells. (BTA-TD)**	12	54.5–68.4	0.6–2.4	14.4–15.8	4.9–10.8	0.2–0.3	0.5–2.5	1.8–5.5	3.8–5.5	1.7–4.2	0.2–1.1	98.8–100.2
Laug.	ISL40x2068[b]	**Snæfells. (BTA-TA)**	8	53.2–66.3	1.0–3.1	13.9–16.6	5.8–12.5	0.2–0.3	0.7–3.0	2.2–6.4	3.7–5.6	2.7–4.1	0.3–1.4	98.2–100.6
Laug.	ISL40x2608[b]	**Snæfells. (TB-TD)**	14	48.3–67.0	0.4–3.4	14.5–16.8	4.8–12.2	0.2–0.3	0.4–4.1	2.3–8.4	3.5–5.4	1.6–3.7	0.1–1.6	95.9–100.8
Laug.	ISL40x2638[b]	**Snæfells. (BTA-TA)**	10	54.0–60.4	1.1–2.5	14.3–16.9	6.3–10.7	0.2-0-3	1.3–2.5	3.2–6.0	3.7–5.4	1.4–3.3	0.4–1.1	96.3–100.2
Laug.	ISL40x2638[b]	**Hekla *4*** [3] **(R)**	8	70.5–75.6	0.1–0.2	12.9–13.7	1.9–2.0	0.1–0.1	0.0–0.0	1.2–1.3	4.4–4.7	2.7–2.8	0.0–0.1	94.6–100.2
Laug.	ISL40x2826	**Snæfells. (BTA)**	31	51.4–57.7	2.3–3.4	13.1–14.8	10.1–12.5	0.3–0.4	1.9–3.5	5.1–7.1	2.3–4.6	2.3–3.9	0.9–1.7	98.0–100.9
Laug.	ISL40x3186	**Snæfells. (TD)**	28	62.5–70.8	0.7–1.1	14.0–16.1	4.3–7.1	0.2–0.3	0.4–1.2	1.3–3.0	3.8–4.9	3.4–5.1	0.1–0.4	98.6–101.2
Laug.	ISL40x4624	**Snæfells. (TA)**	16	57.3–62.2	1.0–1.5	14.8–16.8	6.2–7.8	0.2–0.3	1.2–1.9	3.2–4.4	3.9–5.6	2.8–3.4	0.3–0.7	96.5–100.9
Laug.	ISL40x4754[b]	**Snæfells. (B)**	12	47.5–50.4	3.2–4.6	13.1–15.0	11.7–15.0	0.2–0.3	4.2–4.5	7.9–9.1	3.1–4.1	1.5–1.8	0.8–1.5	98.4–100.3
Laug.	ISL40x5064	**Snæfells. (TB-BTA)**	18	48.9–55.8	2.6–3.9	13.7–14.9	10.1–13.3	0.3–0.3	2.9–4.0	5.3–7.8	1.4–4.8	1.9–3.2	1.0–1.2	97.6–100.6
Laug.	ISL40x5454	**Snæfells. (T–A)**	11	56.8–64.2	1.0–3.9	13.7–16.6	6.0–14.3	0.2–0.3	0.9–6.9	3.0–13.2	1.4–5.5	0.6–3.5	0.3–1.2	97.3–101.3
Laug.	ISL40x5684	**Snæfells. (B)**	14	46.9–49.8	3.3–4.4	13.0–14.8	11.8–14.6	0.2–0.3	4.0–4.5	7.5–8.9	3.4–3.8	1.4–1.9	0.8–1.5	98.0–99.4

[a] Cryptotephra, nonvisible tephra, concentrations identified with radiograph and XRF scan data.
[b] Diffused tephra layers with trace visibility, sampling was assisted with radiograph and XRF scan data.

Table 2
Locations describing Snæfellsjökull tephra from Iceland and Northern Europe as presented in Fig. 1. Geochemical range in select major elements.

	Location	Site name	Medium	Tephra	ID/Date	n =	SiO_2 (wt %)	Al_2O_3 (wt %)	K_2O (wt %)	Total (wt %)	Reference
1	ISL. Snæfellsnes	Site 49	Soil	Sn-1	^{14}C corr.	12	65.7–69.6	15.2–16.0	3.9–4.7	98.3–99.6	This study, see Table S1; Jóhannesson et al. (1981)
	ISL. Snæfellsnes	Site 49	Soil	Sn-2	^{14}C corr.	17	62.9–68.0	14.8–16.8	3.5–4.7	94.7–100.1	This study, see Table S1 Jóhannesson et al. (1981)
2	ISL. Snæfellsnes	Site 52	Soil	Sn-1	^{14}C corr.	14	65.3–70.0	14.7–16.0	3.8–4.7	96.1–99.3	This study, see Table S1 Jóhannesson et al. (1981)
	ISL. Snæfellsnes	Site 52	Soil	Sn-3	8-10 ka BP	20	59.6–67.2	15.2–16.3	2.9–4.2	94.5–99.5	This study, see Table S1 Jóhannesson et al. (1981)
3	ISL. Snæfellsnes	Baulárvallavatn	Lake	Sn-1	BL	9	63.8–67.6	14.9–16.4	3.7–4.4	96.6–99.1	Holmes et al. (2016)
4	ISL. Snæfellsnes	Helgafellsvatn	Lake	Sn-1	HF	13	64.9–67.3	15.7–16.4	3.8–4.3	98.4100.2	Riddell et al. (2024)
5	ISL. Hvammsfjörður	Haukadalsvatn	Lake	Sn-1	HAK02	25	64.6–70.0	13.5–16.2	3.7–5.1	98.1–100.8	Harning et al. (2019)
6	ISL. Vestfirðir	Reykjarfördur	Lake	Sn-1	REY	15	63.9–70.6	14.616.3	3.7–5.0	96.5–100.6	Guðmundsdóttir et al. (2016)
7	ISL. Vestfirðir	N. Eyvindar-fjarðarvatn	Lake	Sn-1	NEY	8	63.6–69.3	14.5–16.4	3.2–4.9	95.698.9	Guðmundsdóttir et al. (2016)
8	ISL. Vestfirðir	Dagverðardalur	Lake	Sn-1	DAG	12	64.2–69.9	14.3–16.3	3.8–5.0	94.6–100.6	Guðmundsdóttir et al. (2016)
9	ISL. Vestfirðir	N. Hvalárvatn	Lake	Sn-1	NHV	12	61.6–68.1	14.7–16.1	3.5–4.8	94.9–97.0	Guðmundsdóttir et al. (2016)
10	ISL. Vestfirðir	Skorarvatn	Lake	Sn-1	SKO	12	64.5–69.4	14.6–16.1	3.7–4.8	97.0–98.8	Guðmundsdóttir et al. (2016)
	ISL. Vestfirðir	Skorarvatn	Lake	Sn-1	SKR	23	63.9–69.7	14.7–16.3	3.2–5.3	97.5–99.0	Harning et al. (2018)
11	ISL. Vestfirðir	Tröllkonuvatn	Lake	Sn-1	TRK	10	63.6–68.8	14.8–16.1	3.7–4.7	96.4–98.8	Harning et al. (2018)
12	ISL. Húnavatnssýsla	Hafratjörn	Lake	Sn-1	HAF	11	64.9–66.4	15.7–16.1	3.8–4.1	96.2–98.6	Tinganelli et al. (2018)
	ISL. Húnavatnssýsla	Hafratjörn	Lake	Sn-2	HAF	8	62.7–71.0	13.3–16.5	2.6–4.6	96.8–99.3	Tinganelli et al. (2018)
13	ISL. Húnavatnssýsla	Tindar	Soil	Sn-2	TIN	19	61.2–67.5	15.3–16.3	3.1–4.4	96.2–99.5	Möckel et al. (2017)
14	ISL. Húnavatnssýsla	Kagaðarhóll	Soil	Sn-1	KAGAV	5	63.1–66.5	13.8–16.3	1.5–4.4	98.2–99.0	Bates et al. (2022)
	ISL. Húnavatnssýsla	Kagaðarhóll	Soil	Sn-2	KAGAV	8	63.0–67.9	15.6–16.4	3.1–4.3	96.8–99.9	Unpublished – See Table S1
15[a]	ISL. Húnavatnssýsla	Kagaðarhóll	P-lake	Sn-2	KAGA	11	61.5–67.9	16.2–16.9	3.0–5.0	100–100	Eddudóttir et al. (2015)
	ISL. Húnavatnssýsla	Kagaðarhóll	P-lake	Other	HUN 5.5ka	7	56.2–56.9	15.5–17.6	1.7–2.6	100–100	Eddudóttir et al. (2015)
16[a]	ISL. Húnavatnssýsla	Stóra Búrfell	Soil	Sn-2	BUR	10	61.9–66.4	16.1–16.8	3.2–5.3	100–100	Eddudóttir et al. (2015)
	ISL. Húnavatnssýsla	Stóra Búrfell	Soil	Other	HUN 5.5ka	7	56.5–58.5	15.5–18.0	1.9–2.3	100–100	Eddudóttir et al. (2015)
17	ISL. Húnavatnssýsla	Barðalækartjörn	Soil	Other	HUN 5.5ka	19	55.7–57.4	15.1–15.9	2.0–3.2	97.9–99.7	Eddudóttir et al. (2016)
18	ISL. Húnavatnssýsla	Neðri Mýrar	Soil	Sn-2	NM	19	62.1–67.7	14.7–16.4	3.0–4.6	97.5–99.2	Unpublished – See Table S1
	ISL. Húnavatnssýsla	Neðri Mýrar	Soil	Other	HUN 5.5ka	8	56.1–57.0	15.2–15.8	1.5–2.6	98.2–100.1	Unpublished – See Table S1
19	ISL. Húnavatnssýsla	Blöndulón	Soil	Sn-1	BL223	–	65.4–67.3	15.7–16.6	3.8–4.1	96.6–100.0	Styrmisson (2020)
20	ISL. NE	Askja	Soil	Other	Tephra X; 3.6ka	28	58.3–67.2	13.0–17.5	3.0–4.2	N.A.	Sigvaldason et al., 1992; Annertz et al., (1985)
21	ISL. N	Svartárvatn	Soil	Sn-1	Sn	6	65.869.3	15.2–16.3	3.9–4.6	N.A.	Larsen et al. (2002)
22	ISL. NE	Lögurinn	Lake	Sn-1	LL	16	62.6–66.5	14.4–15.3	3.9–4.2	100–100	Striberger et al., (2011); Guðmundsdóttir et al., (2016)
23	ISL. Shelf	MD99-2275	Marine	Sn-1	431	2	63.7–65.4	15.2–15.6	4.0–4.5	94.4–97.2	Larsen et al. (2002)
	ISL. Shelf	MD99-2275	Marine	Sn-1	455	2/5	63.6–69.5	14.6–15.9	3.8–4.7	96.8–100.0	Larsen et al., (2002); Guðmundsdóttir et al. (2012)
24	Svalbard	Kongressvatn	Lake	Sn-1	KONG39	28	66.7–70.2	15.1–16.1	4.2–4.7	96.2–99.1	D'Andrea et al., 2012
25	SE. Sammak.	Sammakovuoma	Peat	Sn-1	SB-2	26	63.5–70.6	15.2–18.1	3.2–4.9	98.7–102.0	Watson et al. (2016)
26	SE. Sammak.	Sammakovuoma	Lake	Sn-1	SL-2	19	62.0–70.2	14.7–16.2	3.4–4.7	95.5–100.7	Watson et al. (2016)
27	SE. LBA	Lilla Backsjömyren	Peat	Other	LBA-2; 3.6 ka	8	63.8–67.8	15.2–16.2	3.6–4.3	96.0–99.8	Wastegård et al. (2009)
28	FIN. Kivi	Kivihypönneva	Peat	Sn-1	KIVI 76	1	67.1	15.9	4.0	99.2	Kalliokoski et al. (2023)
29	RUS. White Sea	Vodoprovodnoe	P-Lake	Other	VOD1-4; H	14	62.2–67.1	15.3–17.2	2.9–4.3	96.4–99.9	Vakhrameeva et al. (2020)
30	NO. Lofoten	Borg Bog	Peat	Other	BB26-27; H	31	58.7–69.3	14.5–17.0	1.3–4.0	94.8–100.1	Pilcher et al. (2005)

Sites and corresponding references include: Snæfells. = Fagrahlíð, Fróðárhreppur (Jóhannesson et al., 1981; Steinþórsson, 1967); Svartár = Svartárvatn (Larsen et al., 2002); LB = Lilla Backsjömyren (Wastegård et al., 2009); N.M. = Neðri Mýrar (Eddudóttir et al., 2016/unpublished); ISL40x = this study). Country: ISL. = Iceland; SE = Sweden; FIN. = Finland; RUS. = Russia NO. = Norway. H = historic and P-Lake = palaeo lake. By location; Sn-1 (22); Sn-2 (6); Sn-3 (0); Sn-x (2); Sn-H (4); Sn-Post Landnám (2).

[a] Sites 15 and 16 (Eddudóttir et al., 2015) are all SEM data, not microprobe. Microprobe data for the four tephra layers is presented in the supplementary section.

2.4.2. ^{14}C dating

Macrofossils for ^{14}C analysis were retrieved from residues derived from wet sieving through a 250 μm mesh. Plant material was identified and isolated using tweezers and a binocular microscope. Radiocarbon ages were obtained through accelerator mass spectrometry (AMS) at the Ångström Laboratory, Uppsala University, Sweden. To enhance precision and reduce uncertainty, no dates of bulk sediment samples were used to construct the age-depth model. All radiocarbon ages are either terrestrial and/or aquatic macrofossils (Supplementary Table S2). At several intervals (ISL40x655, 2316, 4181 and 4624) both terrestrial and aquatic macrofossils were dated, with the results giving statistically indistinguishable ages, suggesting minimal lake water and reservoir offset. Radiocarbon ages from key sites are (re-)calibrated with CALIB 8.20 (Stuiver and Reimer, 1993; Table S2).

2.4.3. Tephrochronology and analysis

Twenty tephra samples from Laugarvatn lake cores were extracted from specific horizons identified visually and or via x-ray/XRF data. Tephra samples were cleaned of humic material, sieved (63 and 125 μm), dried, mounted in epoxy, polished and carbon-coated for geochemical analysis. Tephra glass geochemistry was analyzed at the University of Iceland using a JEOL JXA-8230 electron probe micro-analyzer (EPMA). The acceleration voltage was 15 kV, the beam current 5 nA (silicic) or 10 nA (basaltic), with a beam diameter of 5 or 10 μm. The standards A99 (for basaltic tephra), ATHO and Lipari Obsidian (both for silicic and intermediate tephra), were measured prior to, and after, the analyses to verify consistency in analytical conditions (Jarosewich, 2002; Óladóttir et al., 2008; Kuehn et al., 2011). Data were then inspected for, and cleaned of, anomalies and analyses with sums <95 % and >101 % were discarded. Mean and standard deviation electron microprobe data are presented in Table 1 (full datasets in Table S1).

2.5. Age-depth model

A Bayesian age-depth model was created in "Rbacon" (v. 2.5.0; Blaauw and Christen, 2011) using the IntCal20 dataset (Reimer et al., 2020). Model constraints include eighteen ^{14}C ages, six Pu samples of radiometric constrain and two tephra marker layers. The plots were created in RStudio (R version 4.2.13.3.3; R Core Team, 2022). Models were optimized using the mean accumulation rates (acc. mean) of 1.5 yr cm^{-1} and a thickness-value of 25. Additionally, the "slump" function was used on tephra layers exceeding 50 mm (2814–2872 mm and 4276–4750 mm composite depth). The slump function creates an abrupt sediment accumulation within the age-depth model, representing an event characterized by the rapid deposition of a thick tephra layer. Note ^{14}C ages (grey color at 2316 mm) are deemed outliers (too old) and were omitted from the age-depth model (Table S2).

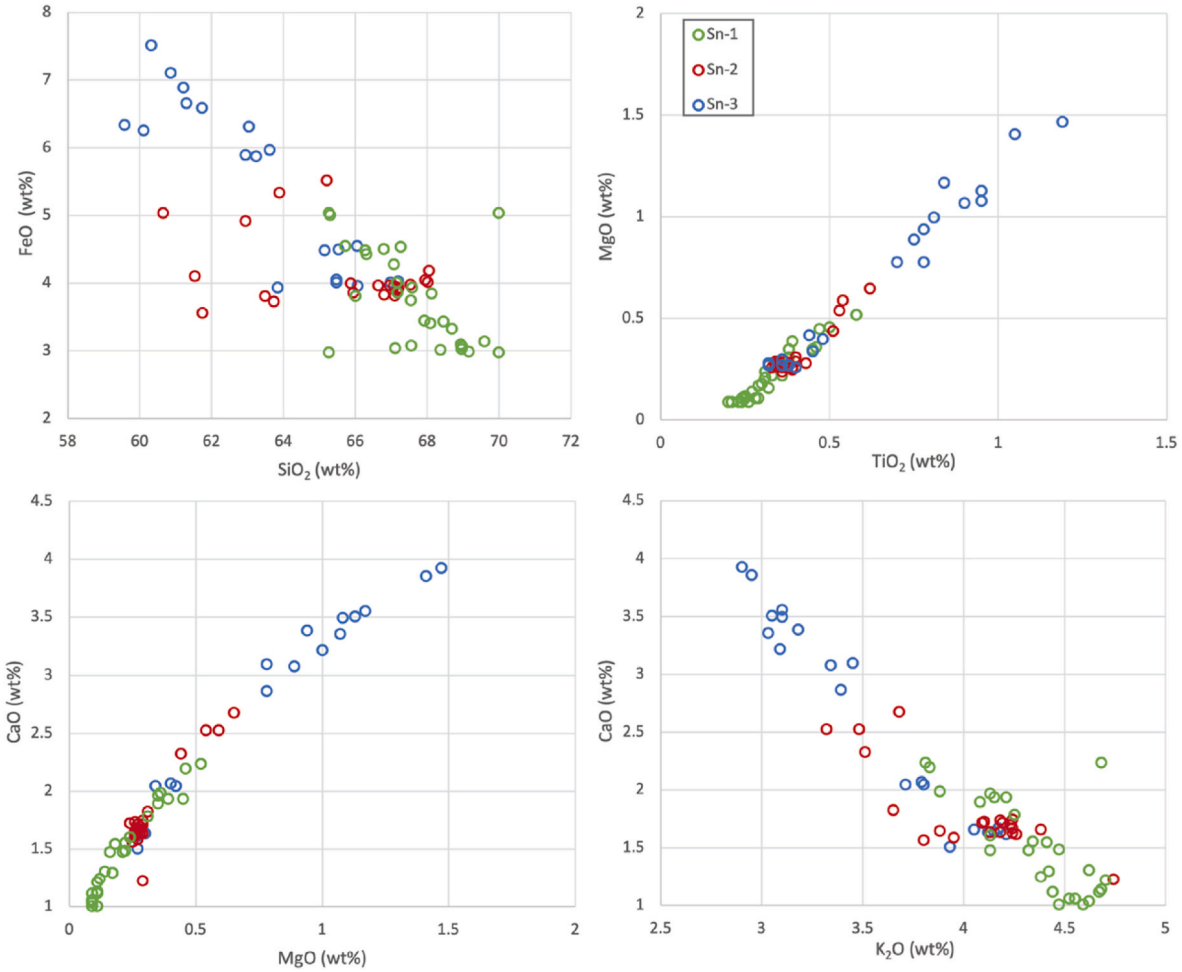

Fig. 3. Selected bi-plots of Sn-1, Sn-2 and Sn-3 tephra sampled from sections on Northern Snæfellsnes peninsula. Note the compositional variations of Sn-3 compared to the younger tephra layers. Full data are provided in Supplementary Table S1.

3. Results

3.1. Description of soil section tephra and geochemistry

3.1.1. Snæfellsjökull Sn-1

A total of 14 and 12 microprobe points analysis were obtained from Sn-1 tephra collected at Sites 49 and 52, respectively. Major elemental compositions of each sample are presented in Table 1. Both samples exhibit SiO_2 values ranging from 65 to 69 wt%, ~15–16 wt% Al_2O_3 and mean K_2O values ~3.9–4.7 wt% (Fig. 3; Table 1). Due to the stratigraphic positioning of the tephra within the sections and the general congruence in geochemical composition, we assume both these tephra layers correspond to the silicic tephra Sn-1 described by Jóhannesson et al. (1981).

3.1.2. Snæfellsjökull Sn-2

A total of 21 microprobe points were analyzed from Sn-2 tephra collected at Site 49 (Table S1). The major elemental compositions are presented for the sample in Table 1. The glass exhibits SiO_2 weight percentage values ranging from ~63 to 68 wt%, 14.8–16.8 wt% Al_2O_3 and K_2O values ~3.5–4.7 wt%. The geochemical composition of Sn-2 is indistinguishable from Sn-1 at this site (Fig. 3). However, due to the stratigraphic positioning beneath Sn-1, we assume these tephra layers correspond to the silicic tephra layer Sn-2 as described by Jóhannesson et al. (1981).

3.1.3. Snæfellsjökull Sn-3

A total of 20 microprobe points were analyzed from the Sn-3 tephra collected at Site 52 (Table S1). The major elemental composition is presented in Table 1. The glass has lower SiO_2 and K_2O contents (~60–67 wt% and ~2.9–4.2 wt%, respectively), than Sn-1 and Sn-2. However, the Sn-3 tephra exhibits a similar Al_2O_3 composition 15–16 wt% (Table 1). The geochemical composition of Sn-3 is distinguishable from Sn-1 (and Sn-2) based on several key elements such as TiO_2, MgO and CaO. The compositional characteristics of Sn-1, Sn-2 and Sn-3 are highlighted in bi-plots and exhibit deviation in Sn-3 composition relative to the younger Snæfellsjökull tephra (Fig. 3).

3.2. Laugarvatn – 76 m a.s.l

Changes in the depositional environment of Laugarvatn are revealed based on variations in lithology, geochemical composition and organic content over the last 10.0 ka (Fig. 4). For simplicity, the Laugarvatn record is classified into two sedimentary lithofacies: gyttja (LF-1) and tephra (LF-2).

3.3. Laugarvatn sediments

3.3.1. Lithofacies 1

LF1 consists of dark brown to reddish (crudely-) laminated silty gyttja with occasionally interbedded silt. LF-1 exhibits a combination of

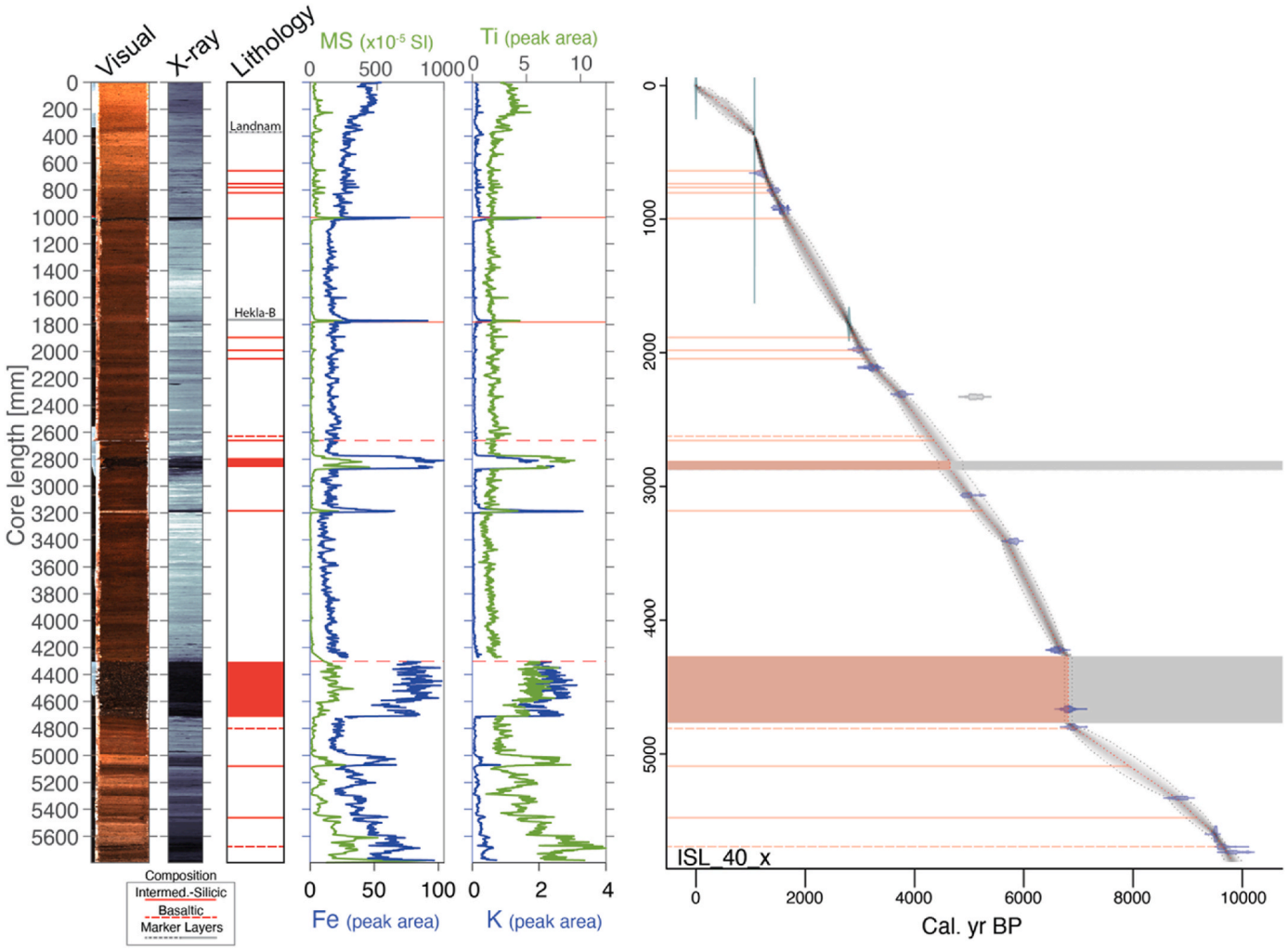

Fig. 4. Stratigraphic data (visual, radiograph, sedimentological log, magnetic susceptibility (MS), normalized titanium, iron and potassium (Ti; Fe; K)) from Laugarvatn. Simplified stratigraphic logs with tephra layers position indicated. Radiocarbon age details listed in Table S3.

low magnetic susceptibility (MS) and titanium (Ti) values with a characteristically low (light) X-ray derived density (Fig. 4). These sediment characteristics are indicative of strata derived from biogenic accumulation with relatively minimal minerogenic input. We interpret LF-1 as the result of predominantly biogenic accumulation deposited within the lake during periods without tephra input or other forms of minerogenic sedimentation, i.e., inflow of glacial meltwater (e.g., Larsen et al., 2015).

3.3.2. Lithofacies 2

LF2 consists of mm to decimeter-scale beds/lamina of high concentration of tephra material. LF-2 is characterized by dark grey to black and light grey to whitish tephra in some cases mixed within beds (salt and pepper). The glass ranges from silt to gravel-size and is characterized by a darkened radiogram (high density), relatively elevated MS values and high Ti-counts indicating minimal organic material. We interpret LF-2 as predominantly volcanic glass originating mostly from primary tephra fall-out from explosive volcanism or proximal effusive eruptions (cf. Jóhannesson, 1977). The transition from LF-1 to LF-2 is often sharp at the lower boundary but can be more gradational and diffused at its upper contact. These transitions are pronounced in the optical image, radiogram and XRF data (Fig. 4). Potassium (K) counts are high in association with silicic tephra layers (e.g. light color tephra layer *c.* 320 cm; Fig. 4). With the aid of the radiograph and XRF scan data, low concentration cryptotephra could be identified and sampled despite not exhibiting visible LF-2 characteristics (e.g., ISL40x375; Landnám; Supplementary Fig. S4). Details of each specific tephra horizon are systematically described in the supplementary section Doc. S2/and in Section 3.5.

3.4. Laugarvatn age-depth model

The age-depth model, spanning the last 10.0 cal ka BP (or spanning the last 10,000 (calendar) years, was constructed from eighteen radiocarbon ages and two tephra marker layers; Landnám tephra and Hekla B (Fig. 4; Table 1 and S1). Td S1). The mean 95 % confidences range is 284 yrs (6–375 yrs in range; Fig. 3). To enhance precision and reduce uncertainty, no dates of bulk sediment samples were used to construct the age-depth model. All radiocarbon ages were measured from either terrestrial and/or aquatic macrofossils (Supplementary Table S2). At several intervals (ISL40x655, 2316, 4181 and 4624) both terrestrial and aquatic macrofossils were dated, with the results giving statistically indistinguishable ages, suggesting minimal lake water and reservoir offset.

3.5. General description of Laugarvatn tephra

Tephra identified within the Laugarvatn lake record range from crypto-tephra (non-visible) layers, recognized and sampled with the aid of the radiographs and the XRF scan data, to coarse beds of glass exceeding 40 cm thickness (Fig. 4; Table 1; Fig. S4). Of the 19s analyzed tephra horizons in the Laugarvatn record, two are correlated to known marker layers, namely ISL40x375 (Landnám, ~877 AD/1073 cal. BP; Larsen, 1984; Schmid et al., 2017) and ISL40x1775 (Hekla B, ~2800 cal. BP; Larsen et al., 2020). Furthermore, a small concentration of tephra characteristic of Hekla 4 can be identified in ISL40x2638. However, given the non-definitive peak in scan data and low concentration of tephra we refrain from defining this as a tephra marker layer or using it in the age-depth model despite its similar age. Fifteen of the remaining 17 tephra layers exhibit evolved glass with geochemical composition characteristic of the Snæfellsjökull volcanic province (Fig. 5; Table 1). The other two layers dominantly exhibit basaltic composition and are also assumed to originate from Snæfellsjökull. We exclude tephra horizons potentially corresponding to Snæfellsjökull marker layers from the age-depth model and independently assess their age.

The Snæfellsjökull marker layers generally exhibit chemistry that ranges from trachy-andesite to trachydacite to rhyolite (~60–70 wt % SiO_2; Fig. 5). The Snæfellsjökull tephra analyzed from the Laugarvatn lake record exhibits similarly evolved chemistry, but the tephra ranges from basalt to rhyolite (~47–70 wt% SiO_2; Fig. 5). Tephra layers from Laugarvatn (and from abroad) often present an internal range in SiO_2 weight percentage (anywhere from 5 to 15 wt% in variation). Accordingly, we present unnormalized geochemical ranges from the major elemental composition of the tephra layers (as average values may not be the most representative; Table 1).

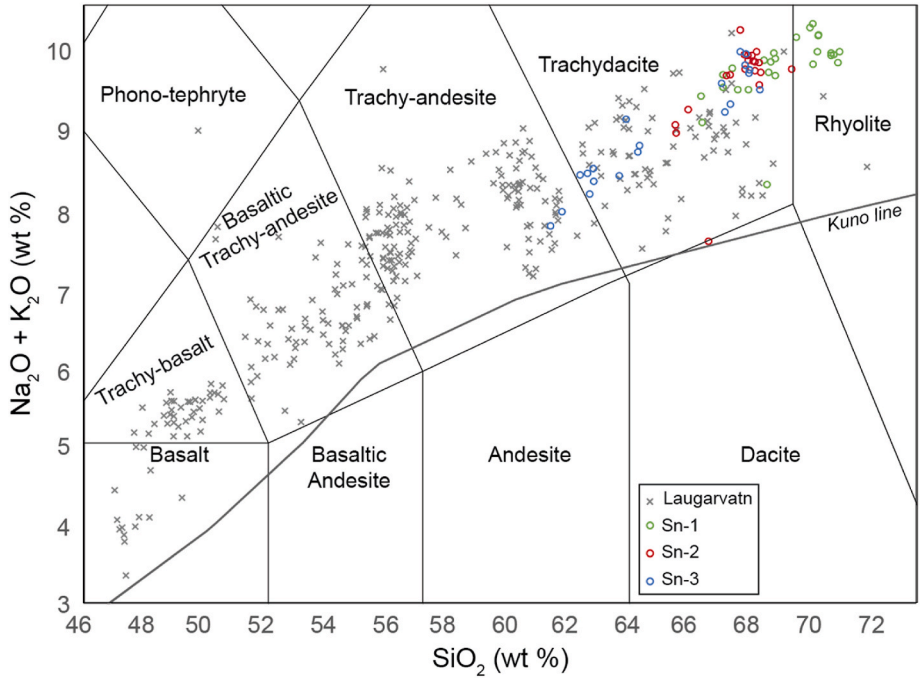

Fig. 5. Total alkali-silica (TAS; Le Maitre et al., 2002) diagram plotting all normalized tephra (excluding Landnám and Hekla B; ISL ISL40x375 and 1775 respectively) analyzed from the Laugarvatn record (grey crosses), in addition to the Sn-1, Sn-2 and Sn-3 tephra sampled from section Sites 49 and 52 (open circles).

We further highlight this range in chemistry through several plots to best depict the potential spread in the composition of the tephra layers (Fig. 6). Notably, reworking and background tephra entering the catchment likely influence these data to some extent. However, we feel this is a more objective means of presenting the results. A detailed description of the Laugarvatn tephra sequence including; characteristics, modeled age (2-sigma range) and probable source for all tephra (base to top) can be found in the supplementary section (Doc. S1).

4. Discussion

4.1. Laugarvatn and Snæfellsjökull volcanic history

The Laugarvatn lake record supplements the stratigraphic mapping conducted along the Snæfellsnes peninsula (Jóhannesson et al., 1981). Isopach contours from Sn-1, Sn-2 and Sn-3 maps are not extended over the lake catchment but trace amounts of tephra have presumably influenced the catchment during these events (due to the lake proximity; Fig. 7). The lake record provides a southerly (and local) perspective to tephra fallout from Snæfellsjökull, recording smaller local effusive volcanic activity and new details to Snæfellsjökull's volcanic history.

4.1.1. Marker layers Sn-1, -2 and -3

Both the prominent stratigraphic nature and age of the ISL40x1013 tephra (less so the geochemistry), are suggestive of Sn-1 tephra deposition into the Laugarvatn lake catchment (Fig. 4). While the roughly 1.5 cm thick salt-and-pepper tephra layer is characterized by SiO_2 dominantly ranging between ~52 and 57 (wt%), it also exhibits glass composition ranging from ~63 to 65 wt % (Table 1). This is notably lower SiO_2 (wt%) than the Sn-1 tephra sampled from the northern half of the peninsula (Site 49 and 52) or any other location where Sn-1 is described (~62–70 wt%; Table 2). The ISL40x1013 tephra layer has a modeled age of 1690 cal. BP (1601–1815), which aligns well with the two previous ages established for the Sn-1 tephra (Fig. 8A; Steinþórsson, 1967; Jóhannesson et al., 1981; Larsen et al., 2002).

While the Sn-2 tephra layer is described from soil sections on the Snæfellsnes peninsula (Jóhannesson et al., 1981) and from the Húnavatnssýsla region in Iceland (Eddudóttir et al., 2015, 2016; Möckel et al., 2017; Tinganelli et al., 2018; Bates et al., 2022), it has not yet been described further afield. Within the Laugarvatn lake record, there is no prominent or light-colored tephra layer coincident with the estimated age of Sn-2 tephra (~4.4 ka BP). There are two tephra layers with similar age to Sn-2 (ISL40x2638; ~4.3 ka BP and ISL40x2866; ~4.7 ka BP). However, these tephra exhibit lower SiO_2 composition (~54–60 and ~51–58 SiO_2 wt%, respectively; Table 1). In addition to the first and only age prescribed to the Sn-2 (Steinþórsson, 1967; Jóhannesson et al., 1981), the deposit is further constrained by radiocarbon ages of twigs in contact with the tephra layer, collected from the Neðri Mýrar section, Northern Iceland (Table S2; Eddudóttir et al., 2016). The ISL40x2638 tephra layer has a modeled age of 4349 cal. ka BP (4148–4575), which aligns well with the previous ages of the Sn-2 tephra from Snæfellsnes, although it is slightly younger than the ages from Húnavatnssýsla (Fig. 8; Table S2; Steinþórsson, 1967; Jóhannesson et al., 1981). However, ISL40x2638 also exhibits a low concentration of rhyolitic glass characteristic of Hekla 4 (4325 ± 8 years BP; Davies et al., 2024). While it is unclear if these shards reflect a peak concentration (layer) in Hekla 4 or are rather background deposition, it does suggest that the stratum is likely younger than Sn-2 given the stratigraphic positioning of the two layers (Doc. S1).

Since the early descriptions and mapping of Sn-3 by Steinþórsson (1967) and then Jóhannesson et al. (1981), correlations have been challenging due to its unknown geochemistry and unprecise age (~8–10 cal. ka BP). However, ISL40x5454 exhibits similar chemistry (to Sn-3 from Site 52) and an age (9.2 cal ka BP) within the 8–10 cal. ka BP

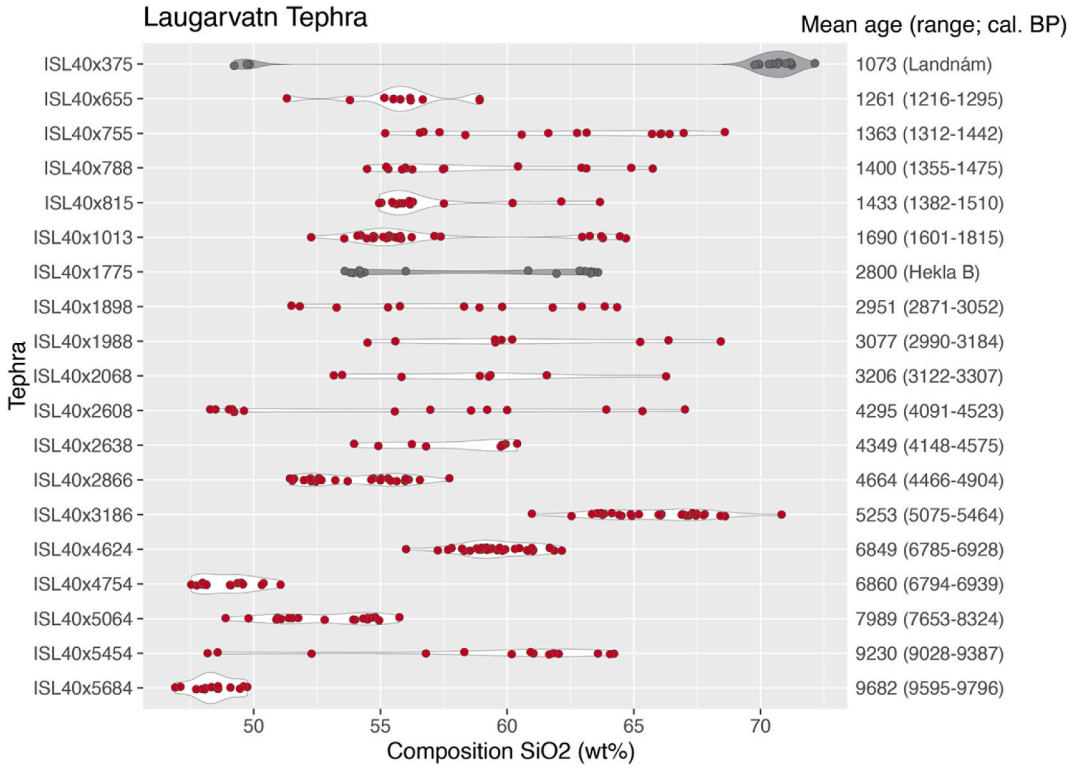

Fig. 6. Violin plots showing the SiO_2 content (wt%) of glass for each tephra layer distributed throughout the Laugarvatn lake record. Note marker layers Landnám and Hekla B are presented in grey color while all tephra attributed to Snæfellsjökull are presented in red. Furthermore, small portion of ISL40x2638 contains rhyolitic shards characteristic of Hekla 4 (Table 1). However, due to the low concentration of rhyolitic tephra, we do not recognize this as a constraining marker layer, albeit acknowledge the geochronological overlap with the Laugarvatn record. (For interpretation of the references to color in this figure legend, the reader is referred to the Web version of this article.)

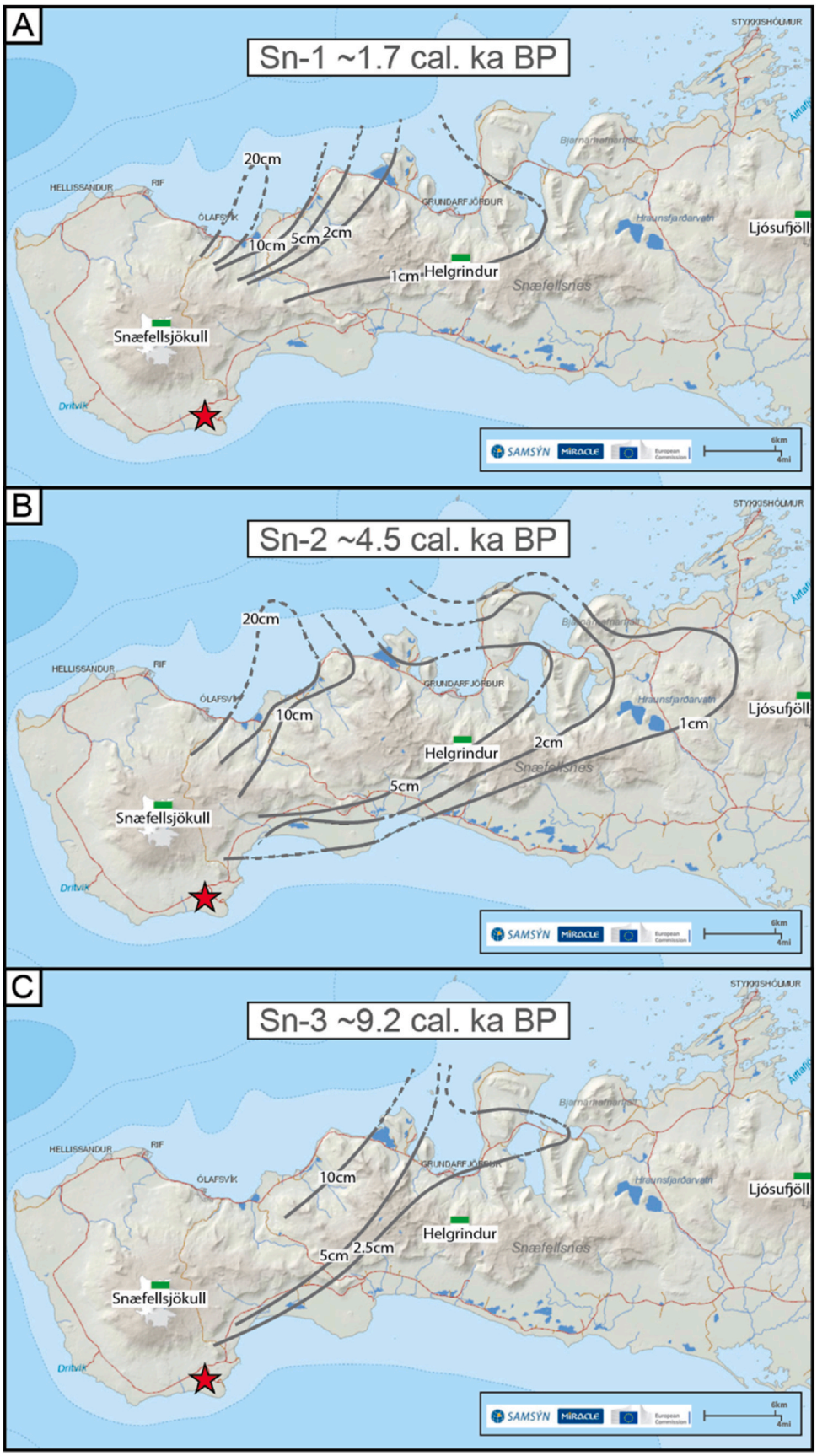

Fig. 7. Isopach maps of Sn-1, Sn-2 and Sn-3 after Jóhannesson et al. (1981) with new age estimates (this study) modified from Icelandicvolcanos.is in relation to Laugarvatn (location indicated by a red star). (For interpretation of the references to color in this figure legend, the reader is referred to the Web version of this article.)

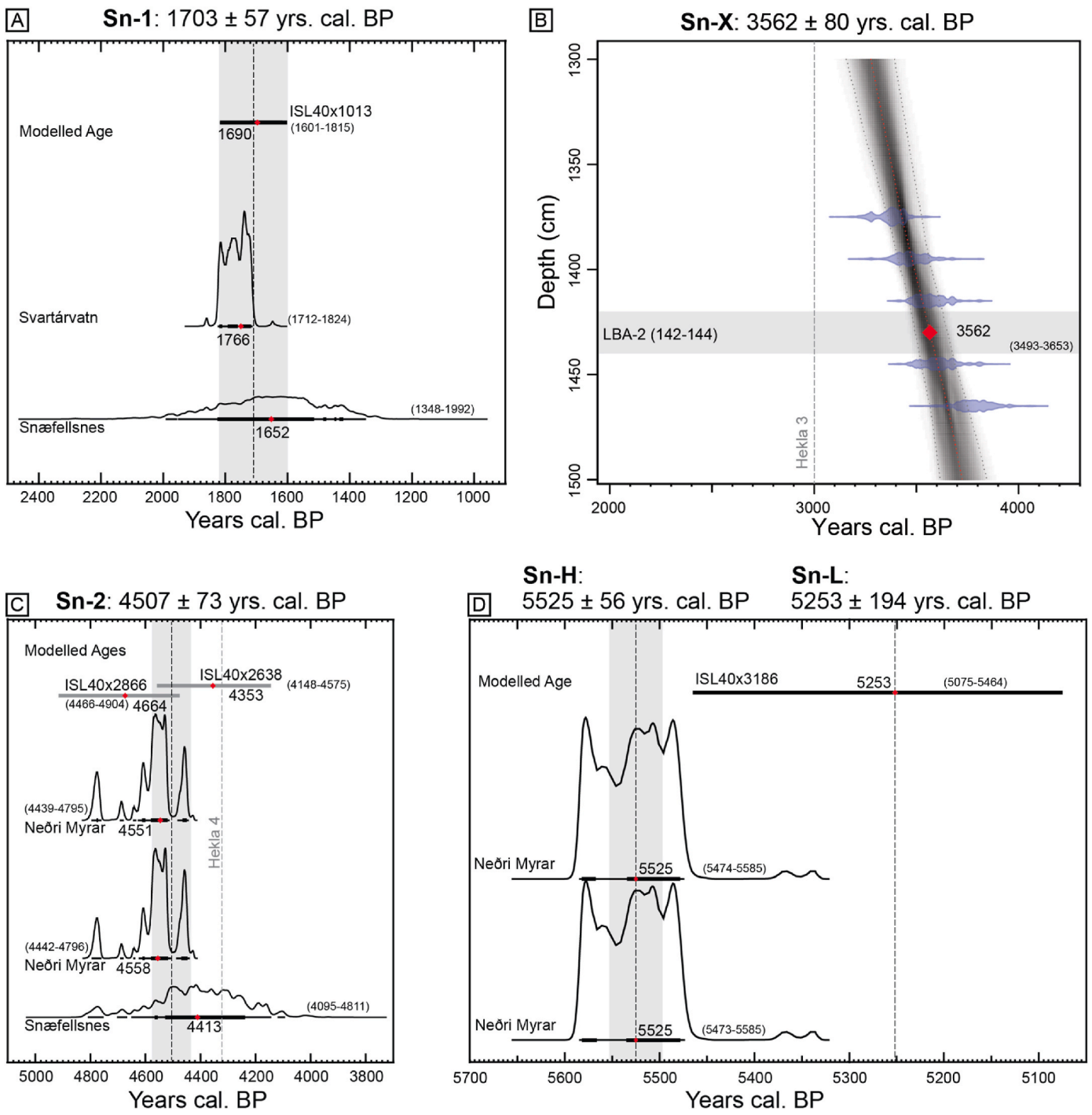

Fig. 8. Mosaic of plots summarizing geochronological constraints on Snæfellsjökull tephra that has been identified, correlated and dated from numerous locations in Iceland and Northern Europe. Radiocarbon age details are presented in Table S2. Modeled ages are derived from the Laugarvatn lake record. Radiocarbon age cumulative probability curves were created in Calib 8.2 (Reimer et al., 2020) while Sn-X tephra age was modeled in RStudio (R version 4.2.13.3.3; R Core Team, 2022). Note the x-axis scale variation on the plots and the reversal on plot B.

estimate proposed by Jóhannesson et al. (1981). Given the similarities, we suggest this is the first time Sn-3 has been described from a lake record (or any stratigraphic record outside the mapping of Jóhannesson et al., 1981). As a result, we effectively date the tephra layer to 9.2 cal ka BP (9028–9387), with the modeled age from the Laugarvatn lake record. Interestingly, while Sn-1 and Sn-2 tephra from Laugarvatn exhibit less silicic composition (compared to what is distally described), the Sn-3 tephra from Laugarvatn exhibits a similar compositional range to what is recorded from Site 52 north of the Snæfellsnes peninsula (Tables 1 and 2).

4.1.2. Potential new marker layers Sn-X, Sn-H and Sn-L

In addition to the three previously described silicic tephra layers from Snæfellsjökull (Jóhannesson et al., 1981), we further discuss three additional tephra, Sn-X, Sn-L and Sn-H, with the potential of widespread deposition and correlation. We summarize their composition (Fig. 9; Table S1), their various correlations (Fig. 10), and their age constraints as well as compare them to modeled ages of tephra from the Laugarvatn

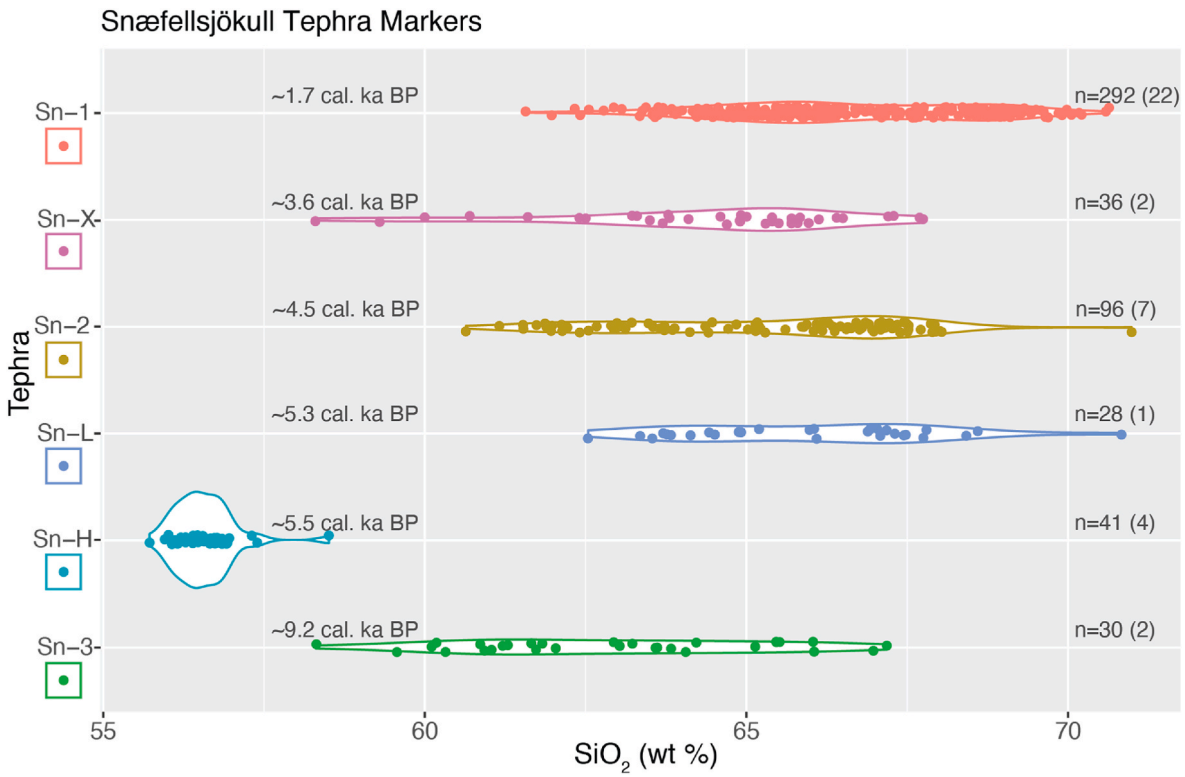

Fig. 9. Violin plots of Snæfellsjökull marker layers Sn-1, Sn-2 and Sn-3, as well as Sn-X, Sn-H and Sn-L, displaying the range in SiO_2 (wt%). Marker layers are presented in stratigraphic order with estimated ages, number of probe points (n = #) and the number of sites (within parenthesis). All probe data are available in Table S1.

record (Fig. 8). We have subdivided all the geochemical data (Table S2) for tephra layers from Snæfellsjökull into these marker layers (Fig. 9) .

The Sn-X tephra has been identified in Iceland (*tephra x*; Annertz et al., 1985; Sigvaldason et al., 1992) and Sweden (*LBA-2*; Wastegård et al., 2009). The Sn-X geochemical composition is like that of Sn-1 and Sn-2 (Fig. 9; Table 1). While the tephra is stratigraphically located between Hekla 3 and Hekla 4 in Iceland, the deposit is best constrained to ~3.6 cal ka BP by the recalibrated age-depth model from Wastegård et al. (2009) derived from the Lilla Backsjömyren (LBA) site in Sweden (Fig. 8B). There are two cryptotephra horizons (ISL40x2068 and ISL40x1988) in the Laugarvatn lake core that have similar trachydacite chemistry, albeit are slightly younger in age, ~3.2 and 3.1 cal ka BP, respectively. It is unclear whether either of these tephra deposits correspond to Sn-X or reflect some phase of volcanic activity following the eruption that deposited the Sn-X tephra.

The Laugarvatn lake record exhibits one distinct silicic tephra layer at roughly 320 cm, (ISL40x3186), which we call Sn-L. The Sn-L tephra (~1 cm thick) is the only white-ish layer visible in the Laugarvatn record and exhibits a trachydacitic composition (ranging from 62.5 to 70.8 SiO_2 wt %; Table 1; Fig. 9). The Laugarvatn age depth model suggests the Sn-L tephra was deposited ~5.3 cal ka BP (5075–5464; Fig. 4; 6). So far, no tephra has been described distally that we can correlate to the Sn-L tephra.

The Sn-H (*HUN*) tephra was first described in Húnavatnssýsla, Iceland (Eddudóttir et al., 2015, 2016). The tephra is constrained to ~5.5 cal ka BP by two radiocarbon ages of twigs in contact with the tephra layers at the Neðri Mýri section, Northern Iceland (Fig. 8; Eddudóttir et al., 2016; Doc. S1; Table S2). While distally deposited Snæfellsjökull tephra generally exhibit composition >60 wt% SiO_2 (and up to 70 wt%), in contrast, the Sn-H displays a homogeneous composition <60 wt% SiO_2 (~56–57.5; Fig. 9). However, the compositional similarities (elevated TiO_2) to Snæfellsjökull tephra are indicative of its origins. At this point, the tephra layer has not yet been described from outside of the Húnavatnssýsla region.

Although similar in age, Sn-L and Sn-H (5.3 and 5.5 cal ka BP respectively; Fig. 8D), exhibit two distinct chemistries (Fig. 9). There are two potential scenarios: the ISL40x3181 tephra is either 1) a new (Sn-L) silicic tephra layer from Snæfellsjökull, yet to be mapped or described, or 2) the deposit reflects deposition from the same, albeit more silicic component, of the Sn-H tephra described from Húnavatnssýsla (Eddudóttir et al., 2016) and would presumably have an age closer to ~5.4 cal ka BP (Figs. 8 and 10). At this point, we favor the first scenario and deem the later less likely.

4.1.3. *Laugarvatn and local effusive volcanism*

While the tephra sampled from the Laugarvatn lake record generally exhibits grain sizes ranging from 63 to 250 μm, one thick (*c.* 40 cm) tephra deposit (at roughly 430 cm) is coarser and stands out from the stratigraphic record (Fig. 3). The thick and coarse nature of the deposit, consisting of fine to gravel size particles (up to 2.5 cm), was challenging to core through and retrieve. The deposit is devoid of visible bedding, exhibiting a massive structure. The tephra has consistent geochemistry from its base to the top of the bed (~57–62 wt% SiO_2) and is believed to have been deposited rapidly ~6.8 cal ka BP (6785–6928). Despite minimal geochronological constraints on the age of the Snæfellsjökull lavas, Kálfatraðahraun (estimated to be between 5 and 8 cal. ka BP), is the only lava that enters the Laugarvatn catchment (Fig. 2; Harðarson, 1993; Kristjánsson et al., 2010). Whole rock geochemistry from the Kálfatraðahraun lava suggests SiO_2 composition of 56.86 wt% and P_2O_5 content of 0.48 wt% (Table S1). The average P_2O_5 for ISL40x4624 is 0.47 wt% (Table S1). Given the thick and coarse nature of the deposit, the approximate age as well as the similarity in whole rock geochemistry, we suggest the ISL40x4624 deposit likely originates from wash-in and local tephra production during the formation of the Kálfatraðahraun lava. This effectively constrains the age of the eruption and lava to *c.* 6.8 cal ka BP.

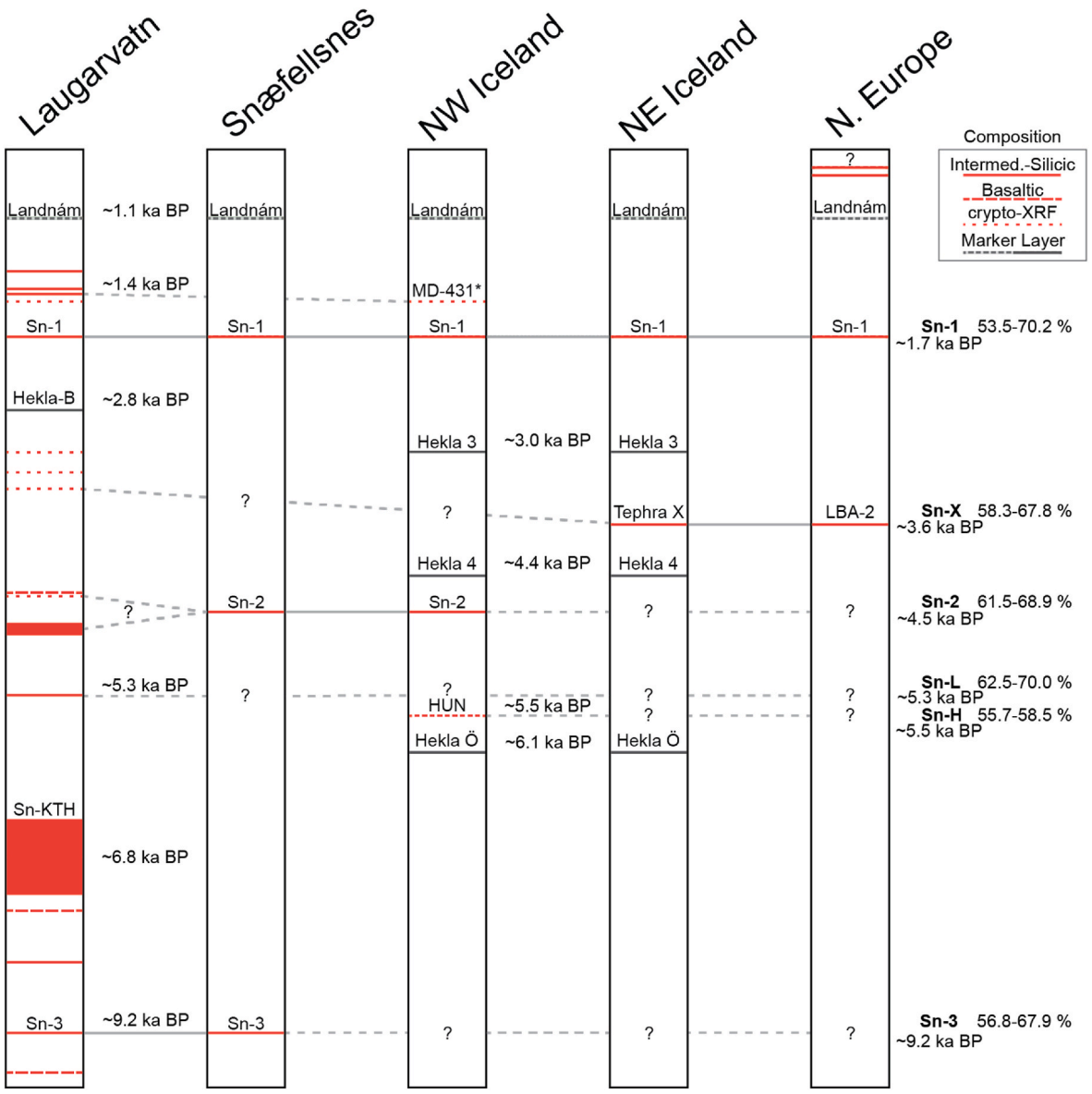

Fig. 10. Correlations of Snæfellsjökull tephra from the Laugarvatn lake record, the Snæfellsnes peninsula (Jóhannesson et al., 1981), N (E and W) Iceland and Northern Europe (Fig. 1; Table 2). Solid and stippled grey lines mark strong and tentative correlation, respectively.

While basaltic lavas flanking Snæfellsjökull have been described and analyzed for whole rock geochemistry (Harðarson, 1993; Kristjánsson et al., 2010), little work has gone into characterizing the basaltic tephra deposits. The Laugarvatn lake record contains three horizons with basaltic tephra: ISL40x5684, 4754 and 2608 (Fig. 6; Table 1). The age of the youngest layer, ISL40x2608, is ~4.3 cal ka BP (4091–4523) and it is partly composed of a distinct basaltic glass component ranging from ~48.0 to 49.5 wt% SiO_2 and a P_2O_5 of ~1.5 wt%. This population of glass exhibits a similar composition to the whole rock geochemistry from the Hnausahraun lava (~48.9 wt% SiO_2 and ~1.1 wt% P_2O_5), which extends over 6 km in length to the sea, roughly 5 km north of Laugarvatn. Accordingly, the age of the Hnausahraun lava is estimated to be between 4 and 5 cal. ka BP (Jóhannesson et al., 1981; Evans et al., 2016), which given the correlation, the Laugarvatn age-depth model further constrains to ~4.3 cal ka BP. The two remaining basaltic tephra layers reflect two (most likely) effusive eruptions dated to 6.9 and 9.7 ka BP according to the age-depth model from Laugarvatn. No correlation to specific lava flows has yet been made.

Together with the Sn-X and Sn-H tephra layers, some 19 potential tephra layers with Snæfellsjökull affinities are presently known. However, of the 17 horizons/layers found in Laugarvatn with Snæfellsjökull affinities there are 6 or 7 horizons that cannot be certified as true tephra layers without additional support from soils sections or lake cores in the Snæfellsnes area. Three horizons dated to 3.0, 3.1 and 3.2 ka show a range of glass compositions without any distinct grouping which raises questions about reworking. Likewise, the four 1.3–1.4 ka tephra horizons detected above the 1.5 cm thick salt-and-pepper tephra layer, representing the 1.7 ka Sn-1, show similarities in the compositional range that could indicate reworking. To resolve this, further work in the area is needed. These 6–7 horizons represent one third of the known tephra record with Snæfellsjökull affinities, which highlights the need for a more detialed investigation on its younger explosive history.

4.2. *Snæfellsjökull-like tephra*

A number of other Icelandic tephra with unknown volcanic provinces (e.g. Hässeldalen, Högstorpsmossen, Ben Goram Moss, Svínavatn SSn) have been tentatively attributed to Snæfellsjökull (Björck and Wastegård, 1999; Boygle, 1999; Langdon and Barber, 2001; Davies et al., 2003). These tephra exhibit a similar evolved composition;

however, we suggest the Hässeldalen, Högstorpsmossen, Ben Goram Moss and Svínavatn SSn tephra layers are unlikely to originate from Snæfellsjökull volcanism. Using the Al_2O_3 wt% as a determining characteristic, as suggested by Wastegård et al. (2018), these layers exhibit unique and distinct chemistry in comparison to all Snæfellsjökull glass data Fig.11).

4.3. Future volcanism from Snæfellsjökull based on its history

Abundant evidence suggests an explosive eruption from Snæfellsjökull about 1800 years ago (~1.7 cal ka BP) deposited tephra across North Iceland, the North Atlantic and Northern Europe (Fig. 10). The widespread tephra Sn-1 has been described from marine, terrestrial and lacustrine archives (although not yet from an ice core), representing a widespread and important Late Holocene marker layer. While Sn-2 (~4.5 cal ka BP - roughly 2.8 ka prior) was previously thought to be the preceding explosive eruption from Snæfellsjökull, it is likely that Sn-X (~3.6 cal ka BP – roughly 1.8 ka prior) is in fact the pen-ultimate (Fig. 10). The Sn-X tephra has been identified in Northeast Iceland (Annertz et al., 1985; Sigvaldason et al., 1992) and Northern Europe (Wastegård et al., 2009), suggestive of a distally deposited explosive eruption (Figs. 1 and 10). While little is known regarding the distal deposition of the Sn-2 or Sn-L tephra, we also note that there are roughly 1700 years between Sn-X (~3.6 ka BP) and Sn-L (~5.3 ka BP).

Results from the Laugarvatn record may suggest that the eruptions producing these widespread marker layers were followed by a period of smaller scale unrest as indicated by a series of subsequent tephra horizons. These findings could indicate more frequent volcanic activity and consequently a shorter (and regular) reoccurrence interval of ~1800 year at Snæfellsjökull. Despite suggestions of a historical eruption(s) from Snæfellsjökull (Pilcher et al., 2005; Plunkett and Pilcher, 2018; Vakhrameeva et al., 2020), we find no evidence of such post-settlement deposits within the Laugarvatn lake record nor elsewhere in Iceland. In summary, the last two distally deposited tephra from Snæfellsjökull occurred roughly 1800 and 3600 years ago. If this pattern is indicative of upcoming activity from the volcanic system, it would not be unusual to experience an eruption from Snæfellsjökull in the near future.

5. Conclusions

- A critical review of (suggested) Snæfellsjökull tephra supplemented with a new high-resolution – well-constrained lake record from Laugarvatn, located proximally on the Snæfellsnes peninsula, suggests the volcanic province may have produced over a dozen explosive eruptions during the last 10 ka BP.
- In addition to the previously described Sn-1 (1.7 cal ka BP), Sn-2 (4.4 cal ka BP) and Sn-3 (9.2 cal ka BP), we introduce three new potential Snæfellsjökull tephra markers, Sn-X (~3.6 cal ka BP), Sn-L (~5.3 cal ka BP) and Sn-H (~5.5 cal ka BP).
- Furthermore, we identified three additional tephra layers (~4.7, ~6.8 and ~8.0 cal ka BP) of dominantly intermediate composition as well as three basaltic tephra layers (~4.3, ~6.9, and ~9.7 cal ka BP) originating from the Snæfellsjökull volcanic province.
- At least two explosive eruptions from Snæfellsjökull have deposited tephra in Northern Europe: Sn-1 roughly 1.7 cal ka BP and Sn-X roughly 3.6 cal ka BP, exhibiting an ~1800-year reoccurrence interval.
- The Sn-1 tephra is an important Late Holocene marker layer deposited across the northern part of Iceland and its shelf area. Furthermore, the deposit is widespread across northwestern Iceland, where Late Holocene Hekla marker layers are less common.
- The Sn-2 tephra exhibits indistinguishable geochemistry from Sn-1, however, it is deposited stratigraphically underneath Hekla 4 (in N Iceland), whereas the Sn-X tephra (also with similar geochemistry) is deposited between Hekla 3 and 4.
- The Sn-3 tephra described by Jóhannesson et al. (1981) has a silicic geochemical composition ranging from ~57 to 64 SiO_2 (wt %), characteristically elevated Al_2O_3 (>15 wt %) and an estimated age of 9.2 ka BP. The Sn-3 tephra exhibits greater wt % of CaO, TiO_2, MgO and FeO than Sn-1 and Sn-2.
- The bi-modal Landnám tephra layer is present in the Laugarvatn record as a cryptotephra and was identified with the use of XRF scan data – by the positive excursion in potassium (K). Despite suggestions of historical eruption(s) from Snæfellsjökull (Pilcher et al., 2005; Plunkett and Pilcher, 2018; Vakhrameeva et al., 2020), no historical tephra from Snæfellsjökull is identified within the Laugarvatn record.
- Despite several Northern European cryptotephra findings with unknown origin (Hässeldalen, Högstorpsmossen; Ben Goram Moss) having similar composition to Snæfellsjökull, we suggest these are unlikely correlations given their absence of characteristically elevated Al_2O_3 (>14 wt %) of Snæfellsjökull tephra.

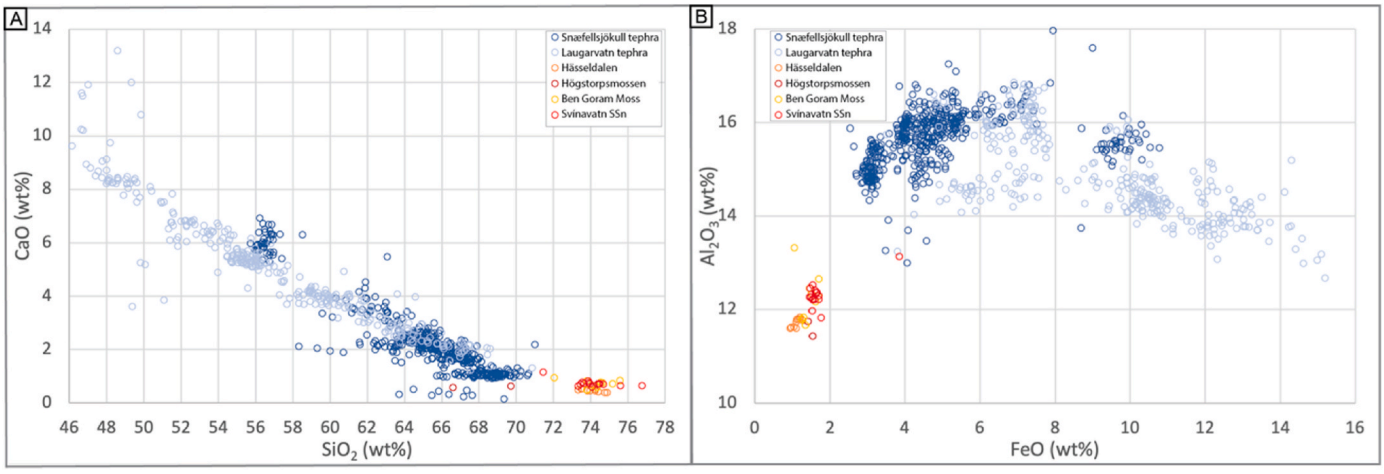

Fig. 11. Biplots comparing weight percentage of (A) CaO verse SiO_2 and B) Al_2O_3 verse FeO) for all Snæfellsjökull tephra (n = 469) with all Laugarvatn tephra (n = 313; excluding Landnám and Hekla B; Tables 1 and 2) compared to four Icelandic tephra of unknown volcanic origin which have been associated with Snæfellsjökull: Hässeldalen (Davies et al., 2003), Högstorpsmossen (Björk and Wastegård, 1999), Ben Goram Moss (Langdon and Barber, 2001) and Svínavatn SSn tephra (Boygle, 1999). While major element compositions for the tephra are generally like Snæfellsjökull (Table S1), they do not exhibit the distinctly elevated Al_2O_3 (dominantly >14 wt%).

Author contributions

Funding acquisition: WRF, KHK. Data collection: WRF, NA, EE, GL, SS, NKL, KHK. Investigation: WRF, SE, EE, GHG, ERG, MK, GL, RHR, AHR, MLSA, NKL. Visualization: WRF. Writing (original draft): WRF. Writing (review and editing): WRF, NA, SB, SE, EE, GHG, ERG, MK, GL, RHR, AHR, MLSA, SS, NKL, KHK.

Declaration of competing interest

The authors declare that they have no known competing financial interests or personal relationships that could have appeared to influence the work reported in this manuscript.

Acknowledgements

This work has been supported by The Carlsberg Foundation (grant CF20-0398 to Farnsworth) within the HM Queen Margrethe II's and Vigdís Finnbogadóttir's Interdisciplinary Research Centre on Ocean, Climate and Society (ROCS). Authors are particularly grateful to Professor Emertius Sigurðar Steinþórsson, for access to a network of whole rock data which he established from the Snæfellsjökull region and was shared with the project. Both Anders J. Hansen and Lasse Vinner are thanked for their support in the field. Authors also kindly acknowledge the constructive and valuable feedback from Prof. Stefan Wastegård and an anonymous reviewer.

Appendix A. Supplementary data

Supplementary data to this article can be found online at https://doi.org/10.1016/j.quascirev.2025.109346.

Data availability

All data and/or code is contained within the submission.

References

Andrade, M., Ramalho, R.S., Pimentel, A., Hernández, A., Kutterolf, S., Sáez, A., Benavente, M., Raposeiro, P.M., Giralt, S., 2021. Unraveling the Holocene eruptive history of Flores Island (azores) through the analysis of lacustrine sedimentary records. Front. Earth Sci. 9, 738178. https://doi.org/10.3389/feart.2021.738178.

Annertz, K., Nilsson, M., Sigvaldason, G.E., 1985. The postglacial history of Dyngjufjöl1. Nordic Volcanol. Inst. Rep. 8503, 1–22.

Bates, R., Erlendsson, E., Eddudóttir, S.D., Möckel, S.C., Tinganelli, L., Gísladóttir, G., 2022. Landnám, land use and landscape change at Kagaðarhóll in northwest Iceland. Environ. Archaeol. 27 (2), 211–227. https://doi.org/10.1080/14614103.2021.1949680.

Björck, J., Wastegård, S., 1999. Climate oscillations and tephrochronology in eastern middle Sweden during the Last Glacial-Interglacial transition. J. Quat. Sci. 14, 399–410.

Björck, S., Ingólfsson, O., Hafliðason, H., Hallsdóttir, M., Anderson, N.J., 1992. Lake Torfadalsvatn: a high-resolution record of the North Atlantic ash zone I and the last glacial-interglacial environmental changes in Iceland. Boreas 21, 15–22.

Blaauw, M., Christen, J.A., 2011. Flexible paleoclimate age-depth models using an autoregressive gamma process. Bayesian analysis 6 (3), 457–474.

Boygle, J., 1999. Variability of tephra in lake and catchment sediments, Svínavatn, Iceland. Global Planet. Change 21, 129–149. https://doi.org/10.1016/S0921-8181(99)00011-9.

Carey, R., Houghton, B.F., þórðarson, T., 2010. Tephra dispersal and eruption dynamics of wet and dry phases of the 1875 eruption of Askja Volcano, Iceland. Bull. Volcanol. 72, 259–278.

Catalogue of Icelandic Volcanos: https://icelandicvolcanos.is/.

Crocker, C., 2023. The first white mother in America, Guðríður þorbjarnardóttir, popular history, firsting, and white feminism. Scand. Can. Stud./Études Scandinaves au Can. 30, 1–28. https://doi.org/10.29173/scancan250.

D'Andrea, W.J., Vaillencourt, D.A., Balascio, N.L., Werner, A., Roof, S.R., Retelle, M., Bradley, R.S., 2012. Mild Little Ice Age and unprecedented recent warmth in an 1800-year lake sediment record from Svalbard. Geol. 40, 1007–1010. https://doi.org/10.1130/G33365.1.

Davies, S.M., Wastegård, S., Wohlfarth, S., 2003. Extending the limits of the borrobol tephra to scandinavia and detection of new early Holocene tephra. Quat. Res. 59, 345–352.

Davies, S.M., Albert, P.G., et al., 2024. Exploiting the Greenland volcanic ash repository to date caldera-forming eruptions and widespread isochrons during the Holocene. Quat. Sci. Rev. 334, 108707.

Denk, T., Grímsson, F., Zetter, R., Símonarson, L.A., 2011. A lakeland area in the late miocene. In: Late Cainozoic Floras of Iceland. Topics in Geobiology. Springer, Dordrecht, 35.

Dugmore, A.J., Sugden, D.E., 1991. Do the anomalous fluctuations of Sólheimajökull reflect ice-divide migration? Boreas 20, 105–113.

Dugmore, A.J., Gisladóttir, G., Simpson, I.A., Newton, A., 2009. Conceptual models of 1200 Years of Icelandic soil erosion reconstructed using tephrochronology. J. North Atlantic 2 (1), 1–18.

Eddudóttir, S.D., Erlendsson, E., Gísladóttir, G., 2015. Life on the periphery is tough: vegetation in Northwest Iceland and its responses to early-Holocene warmth and later climate fluctuations. Holocene 25, 1437–1453.

Eddudóttir, S.D., Erlendsson, E., Tinganelli, L., Gísladóttir, G., 2016. Climate change and human impact in a sensitive ecosystem: the Holocene environment of the northwest Icelandic highland margin. Boreas 45, 715–728. https://doi.org/10.1111/bor.12184.

Einarsson, P., 2008. Plate boundaries, rifts, and transforms in Iceland. Jokull 58, 35–58.

Evans, D.J.A., Ewertowski, M., Orton, C., Harris, C., Guðmundsson, S., 2016. Snæfellsjökull volcano-centred ice cap landsystem, West Iceland. J. Maps 12 (5), 1128–1137. https://doi.org/10.1080/17445647.2015.1135301.

Flores, R.M., 1981. Geological Mapping in Geothermal Exploration with Special Reference to Tephrochronology and Paleomagnetic Techniques. United Nations University, Geothermal Training Programme, pp. 1–78. Report 1981-4.

Foulger, G.R., Doré, T., Emeleus, C.H., Franke, D., Geoffroy, L., Gernigon, L., Hey, R., Holdsworth, R.E., Hole, M., Höskuldsson, Á., Julian, B., Kusznir, N., Martinez, F., McCaffrey, K.J.W., Natland, J.H., Peace, A.L., Petersen, K., Schiffer, C., Stephenson, R., Stoker, M., 2020. The Iceland microcontinent and a continental Greenland-Iceland-faroe ridge. Earth Sci. Rev. 206, 102926.

Guðmundsdóttir, E.R., Eiríksson, J., Larsen, G., 2011. Identification and definition of primary and reworked tephra in Late glacial and Holocene marine shelf sediments off North Iceland. J. Quat. Sci. 26, 589–602.

Guðmundsdóttir, E.R., Larsen, G., Eiríksson, J., 2012. Tephrostratigraphyonthe North Icelandic shelf: extending tephrochronology into marine sediments off North Iceland. Boreas 41, 718–734.

Guðmundsdóttir, E.R., Larsen, G., Björck, S., et al., 2016. A new high-resolution Holocene tephra stratigraphy in eastern Iceland: improving the Icelandic and North Atlantic tephrochronology. Quat. Sci. Rev. 150, 234–249.

Guðmundsdóttir, E.R., Schomacker, A., Brynjólfsson, S., Ingólfsson, O., Larsen, N.K., 2018. Holocene tephrostratigraphy in vestfirðir, NW Iceland. J. Quat. Sci. 33, 827–839.

Hafliðason, H., Eiríksson, J., van Krefeld, S., 2000. Thetephrochronology of Iceland and the North Atlantic region during the middle and late quaternary: a review. J. Quat. Sci. 15, 3–22.

Halldórsson, S.A., Marshall, E.W., Caracciolo, A., et al., 2022. Rapid shifting of a deep magmatic source at Fagradalsfjall volcano, Iceland. Nature 609, 529–534. https://doi.org/10.1038/s41586-022-04981-x.

Harning, D.J., Geirsdóttir, Á., Miller, G.H., Zalzal, K., 2016. Early Holocene deglaciation of Drangajökull, Vestfirðir, Iceland. Quat. Sci. Rev. 153, 192–198.

Harning, D.J., þórðarson, T., Geirsdóttir, A., et al., 2018. Provenance, stratigraphy and chronology of Holocene tephra from Vestfirðir, Iceland. Quat. Geochronol. 46, 59–76.

Harning, D.J., þórðarson, T., Geirsdóttir, Á., Ólafsdóttir, S., Miller, G.H., 2019. Marker tephra in Haukadalsvatn lake sediment: a key to the Holocene tephra stratigraphy of northwest Iceland. Quat. Sci. Rev. 219, 154–170.

Harðarson, B.S., 1993. Alkalic Rocks in Iceland with Special Reference to the Snæfellsjökull Volcanic System. Ph.D. ritgerð, University of Edinburgh, pp. 1–430.

Holmes, N., Langdon, P.G., Caseldine, C.J., et al., 2016. Climatic variability during the last millennium in Western Iceland from lake sediment records. Holocene 26, 756–771.

Jarosewich, E., 2002. Smithsonian microbeam standards. J. Res. Natl. Inst. Stand. Technol. 107, 681–685.

Jóhannesson, H., 1977. þar var ei bærinn, sem nú er borgin. Náttúrufræðingurinn 47, 129–141.

Jóhannesson, H., 1980. Jarðlagaskipan og þróun rekbelta á Vesturlandi. Náttúrufræðingurinn 50, 13–31.

Jóhannesson, H., 1982a. Kvarter eldvirkni á Vesturlandi. Í: Eldur er í norðri. Sigurður Steinþórsson ritstjóri 129–137. Sögufélagið, Reykjavík.

Jóhannesson, H., 1982b. Yfirlit um jarðfræði Snæfellsness. Árbók Ferðafélags Íslands, pp. 151–174.

Jóhannesson, H., 2019. Snæfellsjökull. In: Oladóttir, B., Larsen, G., Guðmundsson, M.T. (Eds.), Catalogue of Icelandic Volcanoes. IMO, UI and CPD-NCIP. Retrieved from. https://icelandicvolcanos.is/?volcano=SNJ.

Jóhannesson, H., Sæmundsson, K., 1998. Geological map of Iceland. 1:500 000. Tectonics. Icelandic Institute of Natural History, Reykjavík.

Jóhannesson, H., Flores, R.M., Jónsson, J., 1981. A short account of the Holocene tephrochronology of the Snæfellsjökull central volcano, western Iceland. Jokull 31, 23–30.

Jóhannsdóttir, G.E., 2007. Mid Holocene to Late Glacial Tephrochronology in West Iceland as Revealed in Three Lacustrine Environments. University of Iceland, p. 170. Unpublished thesis.

Kalliokoski, M., Guðmundsdóttir, E.R., Wastegård, S., Jokinen, S., Saarinen, T., 2023. A Holocene tephrochronological framework for Finland. Quat. Sci. Rev. 312 (108173). https://doi.org/10.1016/j.quascirev.2023.108173.

Kelley, J., Bond, L., Beasley, T., 1999. Global distribution of Pu isotopes and 237Np. Sci. Total Environ. 237, 483–500.
Ketterer, M.E., Watson, B.R., Matisoff, G., Wilson, C.G., 2002. Rapid dating of recent aquatic sediments using Pu activities and 240Pu/239Pu as determined by quadrupole inductively coupled plasma mass spectrometry. Environ. Sci. Technol. 36, 1307–1311.
Ketterer, M.E., Hafer, K.M., Jones, V.J., Appleby, P.G., 2004. Rapid dating of recent sediments in Loch Ness: inductively coupled plasma mass spectrometric measurements of global fallout plutonium. Sci. Total Environ. 322, 221–229.
Kokfelt, T.F., Hoernle, K., Lundstrom, C., Hauff, F., van den Bogaard, C., 2009. Time-scales for magmatic differentiation at the Snaefellsjökull central volcano, western Iceland: constraints from U-Th-Pa-Ra disequilibria in postglacial lavas. Geochem. Cosmochim. Acta 73, 1120–1144.
Kristjánsson, B.R., Valdimarsdóttir, M., Skúlason, S., 2010. Jarðfræði: Viðauki IV með verndaráætlun þjóðgarðurinn Snæfellsjökull. Umhverfisstofnun. Reykjavík, pp. 1–23.
Kuehn, S.C., Froese, D.G., Shane, P.A.R., 2011. INTAV Intercomparison Participants - the INTAV intercomparison of electron-beam microanalysis of glass by tephrochronology laboratories: results and recommendations. Quat. Int. 246, 19–47.
Kylander, M.E., Lind, E.M., Wastegård, S., et al., 2012. Recommendations for using XRF core scanning as a tool in tephrochronology. Holocene 22, 371–375.
Langdon, P.G., Barber, K.E., 2001. New Holocene tephra and a proxy climate record from a blanket mire in northern Skye, Scotland. J. Quat. Sci. 16, 753–759.
Larsen, G., 1984. Recent volcanic history of the Veidivötn fissure swarm, southern Iceland - an approach to volcanic risk assessment. J. Volcanol. Geoth. Res. 22, 33–58.
Larsen, G., 2000. Holocene eruptions within the Katla volcanic system, south Iceland, Characteristics and environmental impact. Jokull 49, 1–28.
Larsen, G., Eiríksson, J., 2008. Late Quaternary terrestrial tephrochronology of Iceland - frequency of explosive eruptions, type and volume of tephra deposits. J. Quat. Sci. 23, 109–120.
Larsen, G., Thorarinsson, S., 1977. H4 and other acid Hekla tephra layers. Jokull 27, 28–46.
Larsen, G., Dugmore, A.J., Newton, A.J., 1999. Geochemistry of historical-age silicic tephras in Iceland. Holocene 9 (4), 463–471.
Larsen, G., Newton, A.J., Dugmore, A.J., Vilmundardóttir, E.G., 2001. Geochemistry, dispersal, volumes and chronology of Holocene silicic tephras from the Katla volcanic system, Iceland. J. Quat. Sci. 16, 119–132.
Larsen, G., Eiríksson, J., Knudsen, K.L., Heinemeier, J., 2002. Correlation of late Holocene terrestrial and marine tephra markers in North Iceland. Implications for reservoir age changes and linking land-sea chronologies in the northern North Atlantic. Polar Res. 21, 283–290.
Larsen, D.J., Miller, G.H., Geirsdottir, A., Ólafsdóttir, S., 2012. Non-linear Holocene climate evolution in the North Atlantic: a high resolution, multi-proxy record of glacier activity and environmental change from Hvítárvatn, central Iceland. Quat. Sci. Rev. 39, 14–25.
Larsen, N.K., Kjær, K.H., Lecavalier, B., Bjørk, A.A., Colding, S., Huybrechts, P., Jakobsen, K.E., Kjeldsen, K.K., Knudsen, K.L., Odgaard, B.V., Olsen, J., 2015. The Response of the Southern Greenland Ice Sheet to the Holocene Thermal Maximum, 43. Geology, pp. 291–294.
Larsen, G., Róbertsdóttir, B.G., Óladóttir, B.A., Eiríksson, J., 2020. A shift in eruption mode of Hekla volcano, Iceland, 3000 years ago: two-coloured Hekla tephra series, characteristics, dispersal and age. J. Quat. Sci. 35, 143–154.
Le Maitre, R.W., Streckeisen, A., Zanettin, B., Le Bas, M.J., Bonin, B., Bateman, P., Bellieni, G., Dudek, A., Efremova, S., Keller, J., Lameyre, J., Sabine, P.A., Schmid, R., Sørensen, H., Woolley, A.R., 2002. Igneous Rocks: A Classification and Glossary of Terms. Recommendation of the International Union of Geological Sciences Subcommission on the Systematics of Igneous Rocks, second ed. Cambridge University Press, Cambridge, p. 236.
Map is Database, 2024. https://map.is/base/.
Möckel, S.C., Erlendsson, E., Gísladóttir, G., 2017. Holocene environmental change and development of the nutrient budget of histosols in North Iceland. Plant Soil 418, 437–457. https://doi.org/10.1007/s11104-017-3305-y.
Newhall, C.G., Self, S., 1982. The volcanic explosivity index (VEI): an estimate of explosive magnitude for historical volcanism. J. Geophys. Res. 87 (C2), 1231–1238. https://doi.org/10.1029/JC087iC02p01231.
Óladóttir, B.A., Larsen, G., þórðarson, Th, Sigmarsson, O., 2005. The Katla volcano S Iceland, Holocene tephra stratigraphy and eruption frequency. Jokull 55, 53–74.
Óladóttir, B.A., Sigmarsson, O., Larsen, G., þórðarson, Th, 2008. Katla volcano, Iceland, magma composition, dynamics and eruption frequency as recorded by tephra layers. Bull. Volcanol. 70, 475–493.
Óladóttir, B.A., Larsen, G., Sigmarsson, O., 2011a. Holocene volcanic activity at Grímsvötn, Bardarbunga and Kverkfjöll subglacial centers beneath Vatnajökull, Iceland. Bull. Volcanol. 73, 1187–1208.
Óladóttir, B.A., Sigmarsson, O., Larsen, G., 2011b. Provenance of basaltic tephra from Vatnajökull subglacial volcanoes, Iceland, as determined by major- and trace element analyses. Holocene 21, 1037–1048.
Pilcher, J.R., Bradley, R.S., Francus, P., Anderson, L., 2005. A Holocene tephra record from the Lofoten islands, Arctic Norway. Boreas 34, 136–156.
Plunkett, G., Pilcher, J.R., 2018. Defining the potential source region of volcanic ash in northwest Europe during the Mid- to Late Holocene. Earth Sci. Rev. 179, 20–37.
R Core Team, 2022. R: A Language and Environment for Statistical Computing. R Foundation for Statistical Computing, Vienna, Austria, 2016. Retrieved from. https://www.Rproject.org/.
Reimer, P.J., Austin, W.E.N., Bard, E., Bayliss, A., Blackwell, P.G., Ramsey, C.B., Butzin, M., Cheng, H., Edwards, R.L., Friedrich, M., Grootes, P.M., Guilderson, T.P., Hajdas, I., Heaton, T.J., Hogg, A.G., Hughen, K., Kromer, B., Manning, S.W., Muscheler, R.J., Palmer, G., Pearson, C., van der Plicht, J., Reimer, R.W., Richards, D.A., Scott, E.M., Southon, J.R., Turney, C.S.M., Wacker, L., Adolphi, F., Buntgen, U., Capano, M., Fahrni, S., Fogtmann-Schulz, A., Friedrich, R., Miyake, F., Olsen, J., Reinig, F., Sakamoto, M., Sookdeo, A., Talamo, S., 2020. The IntCal20 northern hemisphere radiocarbon age calibration curve (0-55 cal kBP). Radiocarbon 62, 725–757.
Riddell, S.J., Erlendsson, E., Eddudóttir, S.D., Gísladóttir, G., Farnsworth, W.R., 2024. A script born of sediment: vegetation and land use at the medieval monastery of Helgafell (Hegafellsklaustur) in western Iceland. Veg. Hist. Archaeobotany. https://doi.org/10.1007/s00334-024-00993-x.
Schmid, M.M.E., Dugmore, A.J., Vésteinsson, O., Newton, A.J., 2017. Tephra isochrons and chronologies of colonisation. Quat. Geochronol. 40, 56–66. https://doi.org/10.1016/j.quageo.2016.08.002.
Sigmundsson, F., Einarsson, P., Hjartardóttir, Á.R., Drouin, V., Jónsdóttir, K., Árnadóttir, T., Geirsson, H., Hreinsdóttir, S., Li, S., Ófeigsson, B.G., 2020. Geodynamics of Iceland and the signatures of plate spreading. J. Volcanol. Geoth. Res. 391, 106436.
Sigmundsson, F., Parks, M., Hooper, A., et al., 2022. Deformation and seismicity decline before the 2021 Fagradalsfjall eruption. Nature 609, 523–528.
Sigurgeirsson, M.Á., Hauptfleisch, U., Newton, A., Einarsson, Á., 2013. Dating of the viking age Landnám tephra in lake myvatn sediment. J. N. Atl. 21, 1–11.
Sigurðsson, H., 1966. Geology of the Setberg area, Snæfellsnes, western Iceland. Soc. Sci. Islandica. Greinar IV (2), 53–125.
Sigvaldason, G.E., Annertz, K., Nilsson, M., 1992. Effect of glacier loading/deloading on volcanism: postglacial volcanic production rate of the Dyngjufjöll area, central Iceland. Bull. Volcanol. 54, 385–392.
Steinþórsson, S., 1967. Tvær nýjar Cl4-aldurs-ákvarðanir á öskulögum úr Snæfellsjökli. Náttúrufræðingurinn 37, 236–238.
Striberger, J., Björck, S., Benediktsson, I.Ö., Snowball, I., Uvo, C.B., Ingólfsson, Ó., Kjær, K.H., 2011. Climatic control of the surge periodicity of an Icelandic outlet glacier. J. Quat. Sci. 26 (6), 561e565. https://doi.org/10.1002/jqs.1527.
Striberger, J., Björck, S., Holmgren, S., Hamerlık, L., 2012. The sediments of Lake Lögurinn - a unique proxy record of Holocene glacial meltwater variability in eastern Iceland. Quat. Sci. Rev. 38, 76–88.
Stuiver, M., Reimer, P.J., 1993. Radiocarbon 35, 215–230.
Styrmisson, Ö., 2020. The roles of abiotic and biotic factors in highland vegetation change near Blöndulón, NW Iceland, 200-2000 CE. Master's Thesis, Faculty of Life and Environmental Sciences. University of Iceland, p. 126.
Tinganelli, L., Erlendsson, E., Eddudóttir, S.D., Gísladóttir, G., 2018. Impacts of climate, tephra and land use upon Holocene landscape stability in Northwest Iceland. Geomorphology 322, 117–131. https://doi.org/10.1016/j.geomorph.2018.08.025.
Vakhrameeva, P., Portnyagin, M., Ponomareva, V., Abbott, P.M., Repkina, T., Novikova, A., Koutsodendris, A., Pross, J., 2020. Identification of Icelandic tephras from the last two millennia in the White Sea region (Vodoprovodnoe peat bog, northwestern Russia). J. Quat. Sci. 35, 493–504, 2020.
Wastegård, S., Andersson, S., Hohl Perkins, V., 2009. A new mid-Holocene tephra in central Sweden. GFF 131, 293–297. https://doi.org/10.1080/11035890903452662.
Wastegård, S., Gudmundsdóttir, E.R., Lind, E.M., Timms, R.G.O., Björck, S., Hannon, G. E., Olsen, J., Rundgren, M., 2018. Towards a Holocene tephrochronology for the Faroe Islands, North Atlantic. Quat. Sci. Rev. 195, 195–214.
Watson, E.J., Swindles, G.T., Lawson, I.T., Savov, I.P., 2016. Do peatlands or lakes provide the most comprehensive distal tephra records? Quat. Sci. Rev. 139, 110–128.
Wright, T.J., Sigmundsson, F., Pagli, C., Belachew, M., Hamling, I.J., Brandsdóttir, B., Keir, D., Pedersen, R., Ayele, A., Ebinger, C., Einarsson, P., Lewi, E., Calais, E., 2012. Geophysical constraints on the dynamics of spreading centres from rifting episodes on land. Nat. Geosci. 5, 242–250.
þorarinsson, S., 1944. Tefrokronologiska studier på Island (Tephrochronological studies in Iceland). Geogr. Ann. 26, 1–217.
þorarinsson, S., 1958. The Öræfajökull eruption of 1362. Acta Nat. Isl. II, 1–100.
þorarinsson, S., 1967. The eruptions of Hekla in historical times. In: Einarsson, T., Kjartansson, G., Thorarinsson, S. (Eds.), The Eruption of Hekla 1947-48 I, 1-177 Societas Scientiarum Islandica, Reykjavík.
þorarinsson, 1981. Greetings from Iceland. Geogr. Ann. 63A, 109–118.
þórðarson, T., Self, S., 2003. Atmospheric and environmental effects of the 1783–1784 Laki eruption: a review and reassessment. J. Geophys. Res. 108. https://doi.org/10.1029/2001JD002042.